HIGHER IRRADIANCE AND PHOTODYNAMIC THERAPY FOR AGE-RELATED MACULAR DEGENERATION (AN AOS THESIS)

BY Joan W. Miller MD

ABSTRACT

Purpose: Photodynamic therapy (PDT) using verteporfin was the first pharmacologic therapy for neovascular age-related macular degeneration and changed the treatment paradigm for a major, blinding disease. The experimental work in the nonhuman primate was essential in developing treatment parameters for verteporfin PDT that could successfully occlude choroidal neovascularization with limited injury to the neural retina. Early in the preclinical primate studies, we hypothesized that higher irradiances could be used for ocular PDT than had been used in dermatology and other applications, which typically utilized an irradiance of 150 to 200 mW/cm^2. We set out to test the feasibility of irradiances up to 1800 mW/cm^2.

Methods: PDT was applied to normal monkey eyes using verteporfin/benzoporphyrin derivative (BPD) (2 mg/kg) mixed with low-density lipoprotein in DMSO, and 692-nm light, with a spot size 1250µm, fluence approximately 50 J/cm^2, and irradiance varying from 150 (treatment time, 6 minutes) to 1800 mW/cm^2 (treatment time, 30 seconds). Photocoagulation lesions were applied using 514-nm and 692-nm laser light without drug, with irradiance of 18,750 to 200,000 mW/cm^2 and spot size of 500 µm. Treatment effect was evaluated by fundus photography, angiography, and light and electron microscopy with collagen denaturation as a marker of thermal injury.

Results: Verteporfin/BPD PDT at irradiances of 150 to 1800 mW/cm^2 showed no collagen denaturation in contrast to photocoagulation lesions without dye (irradiance 10-fold and higher).

Conclusions: Verteporfin PDT could safely be performed at higher irradiances, permitting a clinically practical therapy. Ultimately, clinical trials demonstrated that verteporfin PDT could limit moderate vision loss in neovascular age-related macular degeneration. Although anti-VEGF therapy has replaced PDT as a first-line therapy, PDT may still have a role, perhaps in combination therapies. Further investigations to optimize drug delivery and to better understand the molecular mechanisms of PDT effects in both choroidal neovascularization and retina will improve its application in macular diseases.

Trans Am Ophthalmol Soc 2008;106:357-382

INTRODUCTION

Although photodynamic therapy (PDT) is not a new technique, it has undergone a renaissance with the advent of newer photosensitizers and a more rigorous approach to its investigation in ophthalmology. Most of the early efforts were directed at tumors, but investigators quickly realized that vascular thrombosis played a key role in the efficacy of PDT. Subsequently, several investigators studied the ability of PDT using various photosensitizers to occlude normal and neovascular vessels, including choroidal neovascularization (CNV) in animal models.[1-5] The issue of selectivity of CNV occlusion was not addressed in most of these studies. Treatment parameters for PDT using verteporfin were identified and tested in preclinical models by Drs Evangelos Gragoudas, Joan Miller, and coworkers,[6-11] identifying ranges of drug dose, timing of irradiation, and laser parameters including fluence and irradiation. (See Table 1 for a glossary of definitions.) Much of this work was published during the research and development of the technology. However, a key step in the development of a practical therapy for patients was the hypothesis and subsequent proof that higher irradiances could be used for ocular PDT than had been used in dermatology and other applications. With the success of the preclinical studies, clinical trials were initiated, demonstrating the efficacy and safety of verteporfin PDT for patients with CNV, and verteporfin PDT was approved by the US Food and Drug Administration (FDA) in 2000. More recently, anti–vascular endothelial growth factor (VEGF) therapies have demonstrated improved vision outcomes for patients with this disorder, but there may still be a role for PDT, and research to further improve this therapy is warranted.

TABLE 1. GLOSSARY OF DEFINITIONS USED IN LASER PARAMETER DESCRIPTIONS

Energy (J)	Light energy, in this case the energy produced by the laser at wavelengths of 692 nm or 514 nm, measured in joules
Power or flux (J/sec)	Time rate of energy flow, measured in joules per second. For example, movement of one joule of energy per second is equal to one watt (1 W = 1 J/sec).
Fluence (J/cm^2)	Energy per unit area measured in joules per centimeter squared
Irradiance (W/m^2)	Flux or power incident per unit area upon a surface, measured in W/m^2 or mW/cm^2
Spot size (µm)	Diameter typically used to calculate area (πr^2) of photodynamic therapy application

From the Department of Ophthalmology, Harvard Medical School, and the Retina Service and the Angiogenesis and Laser Laboratories, Massachusetts Eye and Ear Infirmary, Boston.

PHOTODYNAMIC THERAPY FOR AGE-RELATED MACULAR DEGENERATION

PRINCIPLES AND PRACTICE

The goal of PDT is to provide selective destruction of targeted tissue without disruption of surrounding structures. Historically, PDT was pursued as a therapy for cancer, as an alternative to chemotherapy and radiation. More recently, PDT has shown promise as a treatment for neovascularization, particularly CNV.

Type I and Type II Reactions

The drugs used in PDT are activated by light at wavelengths that correspond to the absorption peaks of the particular drug. The molecule is excited to a triplet state, then returns to ground state after giving off energy to other molecules (Figure 1).[12] When energy is transferred to oxygen to create singlet oxygen, the reaction is termed Type II. In the Type I reaction, energy is transferred to other molecules, forming superoxide, hydroxyl, and other free radicals. Type II is the predominant mechanism in PDT, when sufficient oxygen is available in the target tissue. Singlet oxygen reacts over a distance of 0.1 μm, and its effects are therefore limited to the cell in or near which it is generated. Singlet oxygen and other free radicals damage cytoplasmic or mitochondrial membranes or the plasma membrane. This can lead to death of the cell itself or merely alter its properties sufficiently to disrupt the tissue. In the case of endothelium, an altered cell surface can lead to platelet aggregation and thrombosis of the vessel.

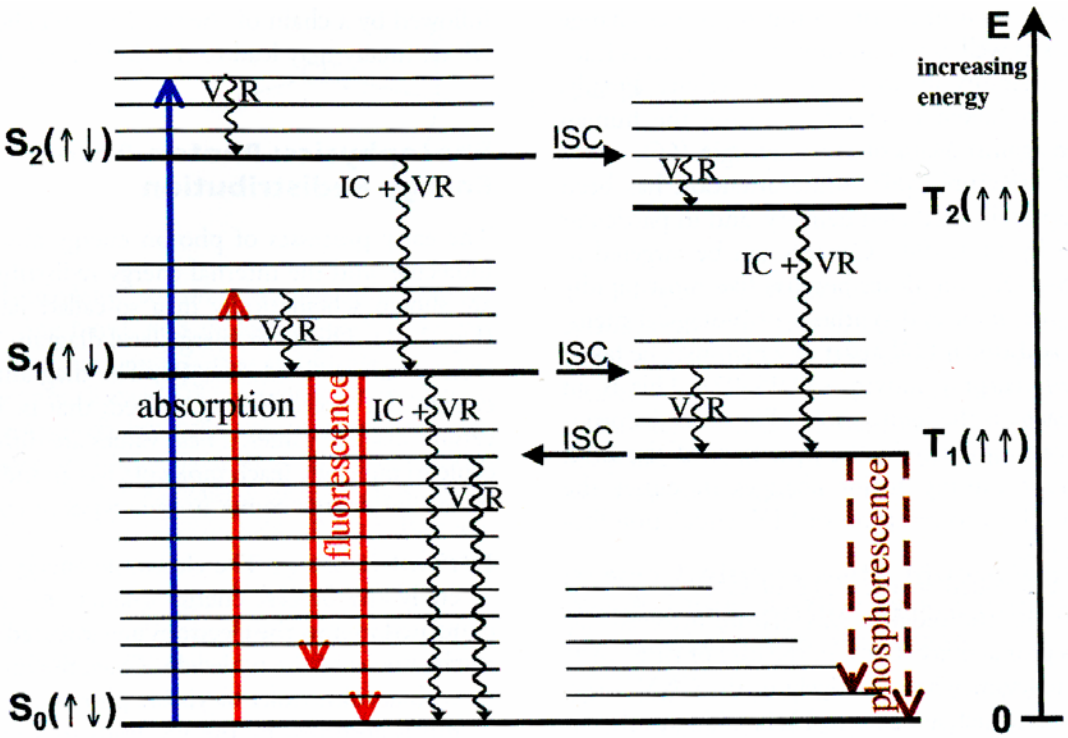

FIGURE 1

The Jablonski diagram. The thick horizontal lines indicate electronic energy levels. S_0, S_1, and S_2 are singlet electronic energy levels of the photosensitizer (PS); T_1 and T_2 are triplet electronic energy levels. The thin horizontal lines represent the vibrational energy levels associated with each electronic state. The blue arrow represents light absorption of a blue (energized) photon. The red upward-pointing arrow represents red (less energetic) light absorption. The red (down-pointing) arrows represent fluorescence (ie, loss of energy) at 2 different wavelengths. The horizontal arrows labeled ISC (intersystem crossing) represent radiationless processes in which the PS goes from a singlet to triplet electronic state or vice versa. This process is generally fast relative to vibrational energy loss by energy exchange with the surrounding molecules. The latter, indicated by VR (vibrational relaxation), are also radiationless processes and indicate energy loss by the PS in the form of heat to the surroundings. The arrows labeled with IC (internal conversion) represent a change in an electronic state (between 2 singlet or 2 triplet states), which is generally followed by vibrational energy. This is followed by vibrational relaxation of the PS molecule and the corresponding heating of the environment. Finally, the dashed red vertical arrows represent a low-probability energy loss process of the PS by emitting phosphorescent photons in the infrared. This is accompanied by a change from the T_1 electronic state to the S_0 ground state. (Reprinted with permission from van den Bergh HE et al.[12])

Multiple factors govern the effectiveness of a given photosensitizer and depend in part on its photophysical and physicochemical properties. The absorption spectrum of the photosensitizer dictates the wavelengths of the radiation that may be suitable for PDT. Generally, the wavelength(s) selected coincides with an absorption maximum of the photosensitizer. The absorption spectrum of several photosensitizers that have been used in ophthalmology are superimposed in Figure 2. The effective penetration depth of the PDT treatment is dependent on the wavelength of the light and the optical properties of the tissue. Typically, the effective penetration depth is 2 to 3 mm at 630 nm, and increases to 5 to 6 mm at longer wavelengths (700 to 800 nm).[13] These values can be altered by changing the biological and physical characteristics of the photosensitizer. In general, photosensitizers absorbing at longer wavelengths, with higher molar absorption at these wavelengths, are more efficient photodynamic agents.[14]

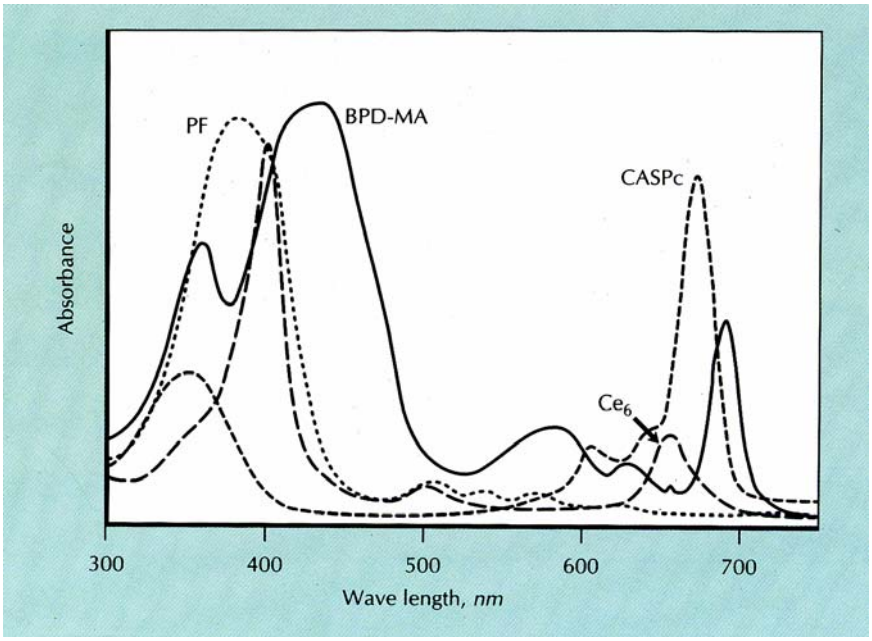

FIGURE 2

Absorption spectra of selected photosensitizers that have been used in photodynamic therapy. PF, photofrin; BPD-MA, benzoporphyrin derivative monoacid; Ce6, chlorin e6; CASPc, chloroaluminum sulfonated phthalmocyanine. (Reprinted with permission from Lui H et al.[84])

Other important aspects of a particular photosensitizer include the metabolism, pH, and route of administration of the photosensitizer. For most ophthalmic applications, photosensitizers are administered intravenously, either as an intravenous infusion or more rapidly as an intravenous bolus injection. A key consideration in PDT is the ability of the photosensitizer to localize preferentially in target tissues, which leads to damage of the target tissue and minimizes collateral damage to surrounding tissues.[15]

Serum proteins are responsible for the transport of photosensitizers to various areas of the body. The binding of the photosensitizer to the various types of serum protein is mainly governed by the degree of hydrophilicity/lipophilicity of the photosensitizer. In general, moderately hydrophobic photosensitizers are transported in the bloodstream preferentially by albumin, whereas highly hydrophobic photosensitizers interact mainly with lipoproteins.[16,17] The amounts of hydrophobic photosensitizer recovered from the different lipoprotein fractions reflect their relative concentration in the serum.[18] In general, high-density lipoprotein (HDL) binds the highest amount of hydrophobic photosensitizers as compared with low-density lipoprotein (LDL) and very low-density lipoprotein (VLDL).[19] VLDL binds less than 10% of the hydrophobic photosensitizer transported by the total lipoprotein fraction.[16,20] Comparing the binding of the various photosensitizers to LDL, the greatest percentage has been found for the highly hydrophobic Zn-phthalocyanine (ZnPc) and tin ethyl etiopurpurin (SnET2).[21]

The use of delivery vehicles for formulation of porphyrin-type photosensitizers was prompted by the observation that the affinity of such photosensitizers for neoplastic and neovascular tissue[22-25] increases with increasing hydrophobicity. The selective biodistribution of these sensitizers is enhanced by their incorporation into amphicilic systems, eg, phospholipid vesicles or oil emulsions, which are stable in an aqueous milieu yet possess apolar compartments where hydrophobic substrates are embedded.[12,26] In general, the use of liposomal vesicles that are in a fluid state at the body temperature of 37°C appears to orient the photosensitizer toward LDL.[27] Some second-generation photosensitizers, eg, SnET2, verteporfin, and ZnPc are currently formulated in lipid-based delivery systems.

One strategy to increase selectivity of tissue delivery is to use lipoproteins. When porphyrin photosensitizers are preincorporated into liposomes or mixed with lipoproteins, their delivery to neoplastic tissues is increased.[20,28-31] Jori and coworkers[32] noted that hematoporphyrin derivative (HPD) was carried primarily by HDL, while Barel and coworkers[30] found that mixing the photosensitizer with LDL in vitro, leading to association rather than actual covalent binding, increased the specificity of delivery to tumor tissue in vivo. This may be due to the fact that cells with high mitotic activity, such as tumor and neovascular endothelial cells, were found to have high-expression of LDL receptors (such as the apo B/E receptor), which might lead to more efficient uptake of LDL-bound molecules by receptor-mediated endocytosis.[23,33,34] Hamblin and coworkers[35] demonstrated that photosensitizers bound to lipoprotein

are taken up in large amounts by cells possessing scavenger receptors and/or phagocytosing activity. In considering selectivity for CNV, it should be noted that retinal pigment epithelial (RPE) cells also have abundant LDL receptors utilized in phagocytosis of photoreceptor outer segments and therefore may be targeted by photosensitizers that utilize LDL.[36-38] The technique of Barel (mixing porphryins and LDL) was applied to benzoporphyrin derivative (BPD) for the treatment of experimental tumors and CNV.[7,39] Photosensitizers may also be retained in tumors due to a larger interstitial space and poor lymphatic network.[40]

Another strategy to increase selectivity is to bind the photosensitizer to an antibody directed at the target tissue.[41] This has been done with some success in experimental tumor models.[42-44] To investigate PDT targeted to CNV, a homing peptide directed to the VEGFR2 receptor, also known as KDR or FLK-1, was chosen.[45] A peptide was utilized because of the ease of synthesis and modification, lack of tissue cross-reactivity, a minimized immunologic reaction, and the potential incorporation of multiple targeting peptides to the photosensitizer-carrier complex. VEGFR2, while not completely selective for CNV, is more highly expressed in neovascular tissue than normal vessels, and the peptide selected, ATWLPPR, had been shown to completely inhibit VEGF binding to VEGFR2.[46] Targeted verteporfin was produced by binding verteporfin to a polyvinyl alcohol (PVA) linker and then to the homing peptide ATWLPPR. The controls used were verteporfin and verteporfin bound to PVA to create a large molecule but without specific targeting properties. PDT using both targeted verteporfin and verteporfin-PVA were found to be effective in CNV closure in the laser-injury model in the rat, and also more effective than commercially available verteporfin. PDT studies performed on normal eyes to assess selectivity revealed that 1 day after PDT using targeted verteporfin there was no angiographic change. Histologic study demonstrated preserved retina with very minimal changes to RPE, consistent with a grade 1 lesion. In contrast, PDT using either verteporfin or verteporfin-PVA showed hyperfluorescence on angiography and retinal damage on light microscopic examination. These studies suggest that targeted PDT using homing peptides to the tissue of interest has great potential to improve the selectivity of treatment.

The subcellular target may also vary among photosensitizers.[47,48] Some photosensitizers cause damage primarily to the plasma membrane and mitochondria, and others cause nuclear or lysosomal damage. Despite evidence for direct damage to tumor cells under some circumstances, most data suggest that occlusion of tumor vasculature is an important mechanism leading to tumor cell death. PDT-induced damage to endothelial cells results in platelet adhesion and degranulation, leading to stasis and aggregation of blood cells and vascular occlusion. After PDT, there is release of eiconasoids, including thromboxane and histamine, as well as tumor necrosis factor (TNF-α), which may contribute to vascular occlusion.[49]

One current area of research in PDT is the molecular basis of cellular responses, including necrosis and apoptosis following PDT.[50] These likely vary among different photosensitizers, with tissue location, and even with dosimetry of drug and light. It is difficult to prove in clinical PDT whether tissue effect is primarily necrosis or apoptosis. Apoptosis is a process of orderly cell suicide, without debris, that occurs in development, in normal tissue, and in response to external insult such as PDT. In contrast, necrosis is a less controlled response, occurring subsequent to ischemia, infection, or other external insult, and results in a marked inflammatory response, tissue destruction, and debris. Another consideration in the action of PDT on CNV is the vascular effect of PDT, which probably results from injury to endothelial cells (including apoptosis and necrosis), with exposure of the basement membrane, platelet activation, leakage through the disturbed vasculature, and clotting secondary to the platelet effect and release of thromboxane and other clotting factors.[12] Although we think of PDT cell damage as a very localized event, there may also be indirect damage as well. For instance, leukocytes may be activated by PDT and may release other factors that cause further damage to tissue. In experimental and clinical CNV, in particular, macrophages play an important role in angiogenesis and could be part of the PDT response. Studies in experimental CNV models have shown morphologic evidence of dose-dependent photoreceptor degeneration.[8,9,51] More recently, it has been demonstrated that verteporfin PDT caused apoptosis of photoreceptors and CNV cells using electron microscopy and TUNEL staining.[50,51] Dephosphorylation of Akt occurred in CNV within 1 hour of PDT, with subsequent caspase activation at 3 hours in TUNEL-positive cells in CNV.[50] TUNEL staining in CNV increased at 3 hours and peaked 6 hours after PDT and, in addition, showed a dose-dependent relationship to verteporfin dose. Macrophages were evident in CNV lesions before PDT but did not increase after treatment. However, macophages appear to play an indirect role in PDT via the enzyme nitric oxide synthase (NOS). Nitric oxide (NO) is generated by the oxidation of arginine, a reaction catalyzed by the NOS, and is an important signaling molecule that mediates multiple physiologic processes, including vasodilation and neurotransmission. Excess NO can mediate tissue injury and can be proapoptotic or antiapoptotic, depending on the biological environment and level of other signals. In particular, NO has been shown to be toxic to photoreceptors.[52-54] NOS has 3 isoforms—endothelial NOS (eNOS), neuronal NOS (nNOS) and inducible NOS (iNOS); the first 2 isoforms are constitutively expressed. Recently, it was found that iNOS was increased in CNV after PDT and was observed in areas with ED-1 positive cells (a marker for macrophages). In addition, a NOS inhibitor reduced photoreceptor apoptosis after PDT without compromising the effect on CNV closure.[51] These data may explain why anti-inflammatory agents combined with PDT improve the clinical results[55-59] and also suggest that adjunctive antioxidant therapy, and specifically, NOS inhibition, may be a useful combination strategy to reduce photoreceptor injury following PDT.

Many light sources can be used for PDT, including broad-band light from incandescent or arc lamps, or monochromatic light from tunable argon-pumped dye lasers or diode lasers. Broad light bands may enhance the photodynamic effect if they excite secondary absorption peaks of the photosensitizer. Slit-lamp delivery of laser light allows for spatial confinement and is particularly suited to intraocular applications.[5,7,8] The laser treatment parameters for PDT are important for its selectivity and include the fluence, or J/cm^2, and the irradiance (or fluence rate) in mW/cm^2, which determines the length of time of the treatment at a particular fluence. The timing of irradiation for PDT, or the time after photosensitizer injection that the light is applied, is also critical for the selectivity of treatment. While a number of approaches have been used to investigate photosensitizer fluorescence, ophthalmology is ideally suited

for demonstrating photosensitizer spatial and temporal localization by fluorescent angiography. Using standard digital fundus cameras and imaging systems, with filters modified to optimize photosensitizer absorption and fluorescence, serial fundus images following intravenous administration of the photosensitizer were obtained (Arbour J, Association for Research in Vision and Ophthalmology [ARVO] meeting, 1998, Abstract; Kramer M, ARVO meeting, 1995, Abstract; Graham K, ARVO Meeting, 1999, Abstract). These images can be analyzed using image software to compare fluorescence in tissues of interest (retinal vessels, CNV, and normal choroid) over time. One can determine whether a photosensitizer localizes to CNV at a time when it is no longer in retinal vessels, determine whether it leaks out of CNV into the subretinal space, and predict the optimal time window for irradiation during PDT. Preclinical and clinical verteporfin angiography is described in the subsequent "Overview of the Development of Verteporfin PDT" section.

Photosensitizers

Several major classes of photosensitizers have been used in vitro and in vivo in animal models for investigations of PDT. Among these agents, the tetrapyrroles, phthalocyanines, texaphyrins, chlorins, and xanthenes have been used for ocular applications (Table 2). Porphyrin derivatives such as HPD and porfimer sodium (Photofrin) were the most widely studied photodynamic agents. HPD is a complex mixture of porphyrins that is synthesized from hematoporphyrin.[60] PDT with HPD is generally performed with 630-nm wavelength light to increase tissue penetration and decrease absorption by other tissue chromophores. Drawbacks of this agent are its small absorption peak at these longer wavelengths (Figure 1) and the prolonged skin photosensitivity lasting 1 month or more after therapy. Porfimer sodium is a partially purified component of HPD that is more potent and produces less skin toxicity than does HPD.[61] Porfimer sodium has been approved for human use in the United States, Canada, Japan, France, Denmark, Finland, Germany, Ireland, the United Kingdom, and the Netherlands for the treatment of esophageal and lung cancer.[62] In the United States, Canada, the United Kingdom, and European Union, Barrett's espophagus may also be treated with this compound. Porfimer sodium is also approved in Canada for the treatment of superficial bladder cancer. In Japan, gastric cancer and cervical cancer and dysplasia can be treated with porfimer sodium.[63] Clinical trials are under way in North America and Europe to evaluate the usefulness of porfimer sodium in several other cancers, including recurrent astrocytoma, recurrent mouth or throat dysplasia, and bile duct, pancreatic, and gall bladder cancers.

TABLE 2. PHOTOSENSITIZERS FOR OCULAR APPLICATIONS*

PHOTOSENSITIZER CLASS	GENERIC OR CHEMICAL NAME	TRADE NAME	CURRENT STATUS
Xanthene derivatives	Rose bengal		Experimental
Tetrapyrrole derivatives	Hematoporphyrin derivative		Experimental
	Porfimer sodium/dihematoporphyrin ether	Photofrin	Experimental
	Benzoporphyrin derivative/verteporfin	Visudyne	Approved
	Tin ethyl etiopurpurin/SnET2/purlytin	Photrex	Phase 3 confirmatory trial under way
	ATX-S10(Na)		Experimental
Texaphyrins	Lutetium texaphyrin		Phase 1/2 studies completed; no further studies under way
Chlorins and bacteriochlorins	Mono-aspartyl chlorin e6		Experimental
	Bacteriochlorin a		Experimental
Phthalocyanines	Chloroaluminum sulfonated phthalocyanine		Experimental
	Zinc phthalocyanine		Experimental

*Some photosensitizers are approved for other medical uses.

The chlorins, bacteriochlorins, and BPDs are newer porphyrin derivatives with favorable properties that have recently been used for PDT (Table 2). Chlorin derivatives such as mono-aspartyl chlorin e6 are effective photosensitizers in animal tumor models.[64] Bacteriochlorin a is a chlorin derivative that has an absorption maximum at 760 nm and a higher molar absorption coefficient compared with HPD.[65] BPD is another modified porphyrin that has an absorption maximum of about 690 nm and is phototoxic in vivo. BPD is rapidly inactivated or cleared from the body with no significant phototoxicity after 24 hours.[66] It has been used to treat ocular neovascularization and tumors, and its safety and efficacy after intravenous administration have been evaluated in human clinical trials of macular degeneration and other diseases (Gragoudas E, ARVO Meeting, 1997, Abstract)[62] and will be discussed in more detail in the "Overview of the Development of Verteporfin PDT" section.

Studies of PDT have been done with SnET2, which absorbs at 664 nm, in experimental CNV (Baumal C, ARVO Meeting, 1996, Abstract).[67] Closure of experimental CNV was achieved with an intravenous dye dose of 1 mg/kg using 665-nm light with an

irradiance of 600 mW/cm^2, fluence of 35 to 70 J/cm^2, and a spot size of 1200 μm, requiring a light exposure of 60 to 120 seconds. Selectivity and the effects on normal retinal structures were not studied. Based on this preclinical work, a Phase 1 trial was initiated using PDT and tin etiopurpurin to treat CNV. A Phase 3, double- masked, placebo-controlled trial was initiated in the fall of 1998, enrolling 900 patients with new subfoveal CNV secondary to age-related macular degeneration (AMD), with a classic component, measuring 3000 μm or less, and best-corrected visual acuity of 20/63 to 20/500. Treatments were performed every 3 months as in the verteporfin PDT clinical studies, using 600 mW/cm^2 and 36 J/cm^2 with 664-nm laser light.[68] Unfortunately, the Phase 3 trials of SnET2 (purlytin), sponsored by Miravant Medical Technologies and Pharmacia, failed to achieve the primary end point of avoiding moderate vision loss. Subsequent subgroup analyses of data from this trial suggested a vision benefit in treating predominantly occult and purely occult AMD lesions (http://salesandmarketingnetwork.com/news_release.php?ID=2000019). Possible FDA approval of SnET2 PDT awaits the outcome of an ongoing Phase 3 confirmatory trial currently under way in Europe (http://salesandmarketingnetwork.com/news_release.php?ID=2007712; www.clinicaltrials.gov, ClinicalTrials.gov identifier: NCT00157976). Other interesting chlorin derivatives include mono-l-aspartyl chlorin e6 (Npe6) and ATX-S10, which have been used to occlude ocular vessels. Mori and colleagues (Mori K, ARVO Meeting, 1996, Abstract) demonstrated occlusion of choroidal vessels and CNV in Japanese monkeys (*Macaca fuscata*) eyes using 0.5 to 10 mg/kg of Npe6 and 664-nm light (0.4 to 225.0 J/cm^2). Using a dose of 2 mg/kg, Kazi and associates[69] evaluated different fluence rates and times of irradiation in pigmented and nonpigmented rabbits; vessel closure was observed after treatment in pigmented rabbits at a fluence as low as 2.65 J/cm^2. Obana and colleagues (Obana A, ARVO Meeting, 1996, Abstract) used ATX-S10, a new chlorin derivative, to occlude choriocapillaris and choroid in rabbits and rats, using 2 to 12 mg/kg, and 672-nm light at 3.5 J/cm^2. However, in subsequent studies, recurrence and retinal vessel damage were seen in many cases.[70-72] Compared with HPD, these newer-generation photosensitizers share important characteristics, such as higher absorption peaks at longer wavelengths and diminished phototoxicity.

Phthalocyanines are another class of photosensitizers with a strong absorption band at 675 nm.[73,74] Central metals such as zinc and aluminum are incorporated into their structure to increase the triplet state and singlet oxygen yields. Their solubility and cellular localization are at least partially determined by the number and charge of their side chains. The phthalocyanines are cleared more rapidly and produce substantially less skin toxicity than HPD, porfimer sodium, or dihematoporphyrin ether.[74] Phthalocyanines have been investigated in experimental models of ocular neovascularization and ocular tumors, but their safety for use in humans has not yet been determined.[2,3,75]

Texaphyrins are pure, synthetic water-soluble macrocycles that are formulated with central metallic ions. Lutetium texaphyrin (Lu-Tex) is a synthetic, water-soluble macrocycle, with a central metallic ion (lutetium), absorbing at 732 nm. Its efficacy has been demonstrated in the treatment of experimental tumors and atheromatous plaques, and it has been studied in Phase 1 trials of patients with metastatic cancer.[76,77] Preclinical studies demonstrated its utility for angiography and for selective occlusion of CNV, and a Phase 1 and 2 study was undertaken in Lausanne, Switzerland, and in the United States. However, while safe, the efficacy results were not sufficient to justify further clinical trials (Arbour J, ARVO Meeting, 1999, Abstract; Blumenkranz M, ARVO Meeting, 1998, Abstract; Graham K, ARVO Meeting, 1999, Abstract).[78,79]

Xanthene derivatives also have photosensitizing properties.[80,81] Rose bengal is a halogenated fluorescein derivative with increased singlet oxygen yields and photosensitizing ability that has been used to produce photochemically mediated vascular damage of ocular vessels including CNV.[1,5,82,83]

PRECLINICAL EVALUATION OF PDT FOR CHOROIDAL NEOVASCULARIZATION—HIGHER IRRADIANCE STUDIES

INTRODUCTION

Preliminary studies using BPD dissolved in dimethyl sulfoxide (DMSO) and mixed with LDLs demonstrated the potential of PDT to close experimental CNV with limited damage to other retinal structures. The first experiments were carried out using an irradiance of 150 mW/cm^2; irradiance (mW/cm^2) determines the duration of time required to deliver a given fluence. Typically, PDT was performed at irradiances of ≤200 mW/cm^2 in order to avoid thermal damage and, in some instances, pain during treatment. Verteporfin PDT in dermatology trials utilized 120 to 150 mW/cm^2.[84] Higher irradiances were thought to be unsafe or even ineffective. Regardless, PDT at this irradiance (150 mW/cm^2) required treatment times over 10 to 15 minutes, which were judged impractical for treating CNV in clinical practice.[7] We hypothesized that higher irradiance might be permissible in treating choroidal vessels including neovascularization and designed a series of experiments to test this hypothesis in normal eyes. We evaluated PDT using higher irradiances to determine if there was a substantial thermal effect and used disruption of collagen fibrils detected by electron microscopy as a marker of significant thermal damage. Preliminary results of this experiment were presented at the 1993 annual ARVO meeting (Moulton RS, ARVO Meeting, 1993, Abstract). Additional experiments demonstrated the utility of this approach in CNV and elaborated dosimetry and long-term effects.[8,11] A list of publications and the previously unpublished findings presented here are summarized in Table 3.

METHODS

All animal experiments were carried out under the guidelines established by the Association for Research in Vision and Ophthalmology and used protocols approved by the Animal Care Committee of the Massachusetts Eye and Ear Infirmary. A single cynomolgus monkey weighing 3 to 4 kg was anesthetized for all procedures with intramuscular ketamine hydrochloride (20 mg/kg),

diazepam (1.0 mg/kg), and atropine sulfate (0.125 mg/kg). Supplemental anesthesia of ketamine hydrochloride (5 to 6 mg/kg) was given as needed. Proparacaine hydrochloride (0.5%) was used for topical anesthesia, and pupils were dilated with 2.5% phenylephrine hydrochloride and 0.8% tropicamide. The animal was sacrificed with an intravenous injection of pentobarbital sodium (25 mg/kg).

TABLE 3. STUDIES OF PHOTODYNAMIC THERAPY (PDT) WITH BPD/VERTEPORFIN (PREVIOUSLY PUBLISHED AND CURRENT STUDY)

CATEGORY	STUDY DESCRIPTION	STUDY
Previous work, published	Bolus BPD-LDL PDT of CNV at standard and higher irradiance (150-600 mW/cm^2)	Miller[7].
	Bolus liposomal BPD at 600 mW/cm^2, varying other laser and dye parameters in normal choroid and CNV	Kramer[8]
	Slow infusion liposomal BPD (PDT of CNV at 600 mW/cm^2)	Husain[9]
	Long-term effects of liposomal BPD at 600 mW/cm^2 in choroid and CNV	Husain[11]
	Repeated PDT of choroid and optic nerve with liposomal BPD infusion at 600 mW/cm^2	Reinke[6]
	Angiography results	Gragoudas ES, Miller JW, Zografos L, eds. *Photodynamic Therapy of Ocular Diseases.* Philadelphia: Lippincott, Williams & Wilkins; 2004
Unpublished findings	BPD-LDL at higher irradiances in choroid and CNV	Miller [7] and Current study
	Liposomal BPD using higher fluence, higher irradiances in choroid and CNV	Kramer [8], Husain [9], and Current study

BPD, benzoporphyrin derivative; CNV, choroidal neovascularization; LDL, low-density lipoprotein.

Photography

Fundus photography and fluorescein angiography were performed with a fundus camera (Canon Fundus CF-60Z Camera, Lake Success, Long Island, New York). Angiography was performed with 0.1 mL/kg body weight of 10% fluorescein sodium via saphenous vein injection.

Photosensitizing Dye

Initial experiments were carried out using BPD-MA dissolved in DMSO rather than liposomal BPD (verteporfin) that was being used in clinical trials in dermatology, because the manufacturer had supplies sufficient only for the ongoing dermatology clinical trials. To mix BPD-MA with LDL, BPD-MA in doses ranging from 1 to 2 mg/kg was dissolved in DMSO at a concentration of 4 mg/mL.[7,30] Dulbecco's phosphate-buffered saline solution (Meditech, Washington, DC) was then added to the stock to achieve a final BPD–monoacid ring A (BPD-MA) concentration of 0.8 mg/mL. Human LDL was prepared fresh according to the method of Rudel and associates.[85] The protein fraction of the LDL extract was measured using the method of Lowry, and LDL extract was added at a BPD-MA protein ratio of 1:2.5 in milligrams. The dye and dye solutions were protected from light at all times. After mixing, the dye preparation was incubated at 37°C before intravenous injection. For the irradiance experiments described, the drug was administered intravenously over 5 minutes via a saphenous vein, at a dose of 2 mg/kg.

Histology

Eyes were enucleated under deep anesthesia and fixed overnight in modified Karnovsky fixative, and then transferred to 0.1 mol/L cacodylate buffer, at a pH of 7.4 at 4°C. For examination, tissue samples were postfixed in 2% osmium tetroxide and dehydrated in alcohol, embedded in epoxy resin (Epon), and sectioned at 1 µm. For light microscopy, sections were stained with toluidine blue and examined with a photomicroscope (Axiophot, Zeiss, Oberkochen, Germany). For electron microscopy, sections were stained with aqueous uranyl acetate and Sato's lead stain, and examined with a transmission electron microscope (Philips CM10, Eindhoven, The Netherlands). For the higher-irradiance experiments, specific examination of collagen fibrils within the choroid was carried out, and denaturation of collagen fibrils indicated thermal damage that was unacceptable.

Laser Photocoagulation and PDT

Laser photocoagulation lesions were placed in the fundus to compare to PDT lesions using 514- and 692-nm wavelength light. Laser irradiation for PDT was initially performed using 692-nm light from an argon/dye laser delivered via a slit-lamp delivery system with a spot size of 1250 μm. For photocoagulation lesions, the spot size was 500 μm. For the PDT irradiance experiments, the fluence was near 50 J/cm^2 and the irradiance varied between 150 mW/cm^2 and 1800 mW/cm^2, producing a range of treatment times from 6 minutes to 30 seconds, respectively. Treatment effect was evaluated using fundus photography and fluorescein angiography immediately after laser irradiation, and enucleation at 2 hours after laser treatment with histologic examination with light and electron microscopy.

Table 4 provides the parameters for each laser lesion (see also Figure 3, right).

TABLE 4. PARAMETERS USED TO PRODUCE 514- AND 692-NM ARGON DYE LASER LESIONS IN MONKEY FUNDUS

LESION	WAVELENGTH (nm)	DYE PRIOR TO IRRADIATION	SPOT SIZE (μm)	IRRADIANCE (mW/cm^2)	DURATION OF IRRADIATION (sec)
A	514	No	500	200,000	0.2
B	514	No	500	150,000	0.5
C	514	No	500	75,000	0.5
D	514	No	500	37,500	1.0
E	514	No	500	25,000	1.5
F	514	No	500	18,750	2.0
G	692	No	500	150,000	0.5
H	692	No	500	75,000	0.5
I	692	No	500	37,500	1.0
J	692	No	500	18,750	2.0
K	692	Yes	1250	1,800	30
L	692	Yes	1250	1,200	45
M	692	Yes	1250	600	90
N	692	Yes	1250	300	180
O	692	Yes	1250	150	360

Lesions Produced With 514-nm Light Only (lesions A through F). Laser photocoagulation lesions were sequentially placed in the macula beginning with a standard power used in panretinal photocoagulation (200 mW and spot size of 500 μm to yield an irradiance of 200,000 mW/cm^2). The irradiance was reduced to 150,000 mW/cm^2 and then decrementally reduced until irradiation produced no observable effects at 18,750 mW/cm^2. This series of photocoagulation lesions was utilized as a positive control to demonstrate thermal damage histologically.

Lesions Produced With 692-nm Light Only (lesions G through J). The same procedure for photocoagulation in the macula was performed, this time using light at the wavelength corresponding to an absorption peak for BPD. Beginning at 150,000 mW/cm^2, the power was halved until the irradiation produced no clinical changes at 18,750 mW/cm^2. These lesions were used to contrast and compare thermal burns from 692-nm light with analogous burns made with 514-nm light.

Lesions Produced With 692-nm Light and BPD-MA (lesions K through O). As noted above, standard PDT utilized irradiances at or below 200 mW/cm^2. In these higher-irradiance experiments, we tested irradiances of 1800, 1200, 600, 300, and 150 mW/cm^2, corresponding to treatment times of 30, 45, 90, 180, and 360 seconds, respectively. The total energy delivered was held constant at 54 J/cm^2. All spots were placed in the fundus within 30 minutes of the end of intravenous BPD administration.

RESULTS

In the PDT lesions (150 to 1800 mW/cm^2) using BPD-MA and 692-nm light, no visible changes were noticed acutely, even at the highest irradiance (Figure 3, left). However fluorescein staining was evident on angiography at 1 hour posttreatment at all levels of irradiance (Figure 4). For the lesions without BPD, clinically detectable thermal burns became apparent only at irradiances at or above 37,500 mW/cm^2 (Figure 3, left), and these showed staining on fluorescein angiography (Figure 4). Histopathology of these lesions revealed marked disruption of the outer retina and RPE (Figure 5, top). Thrombosis was seen in the choriocapillaris with larger choroidal vessels appearing patent. Ultrastructural examination confirmed the damage to endothelium of the choriocapillaris and RPE (Figure 5, middle). Fibrils of denatured collagen consistent with thermal damage were evident at lower and higher magnification (Figure 5, bottom) around a choriocapillary with evidence of thrombosis. Clinical, angiographic, and histologic findings were similar for lesions made with 514-nm or 692-nm light (without BPD-MA).

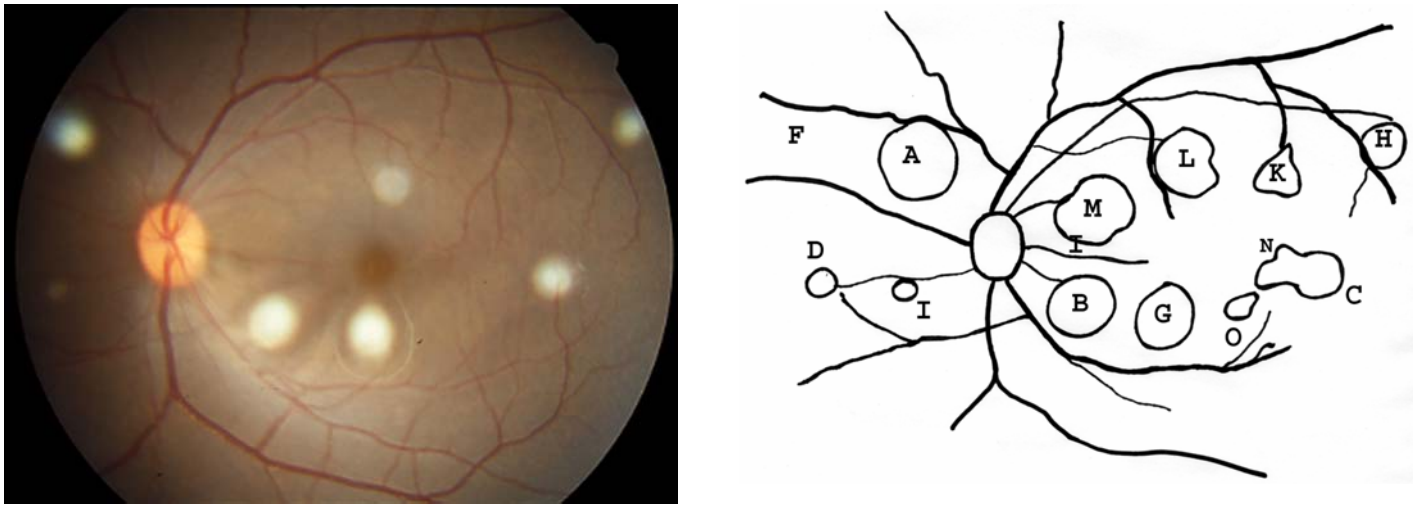

FIGURE 3

Left, Color fundus photograph after laser irradiation. Lesions show varying tissue effect from no apparent change to mild outer retinal whitening, to intense retinal whitening with subretinal fluid. Right, Schematic diagram indicating the laser lesions. For ease of correlation, the shape drawn matches the shape seen in the late frame of the fluorescein shown in Figure 4, right. Nasal lesions are indicated, although they are not captured in the angiogram frames, and only 2 of 3 are seen in the color fundus photograph. The treatment parameters are shown in Table 4.

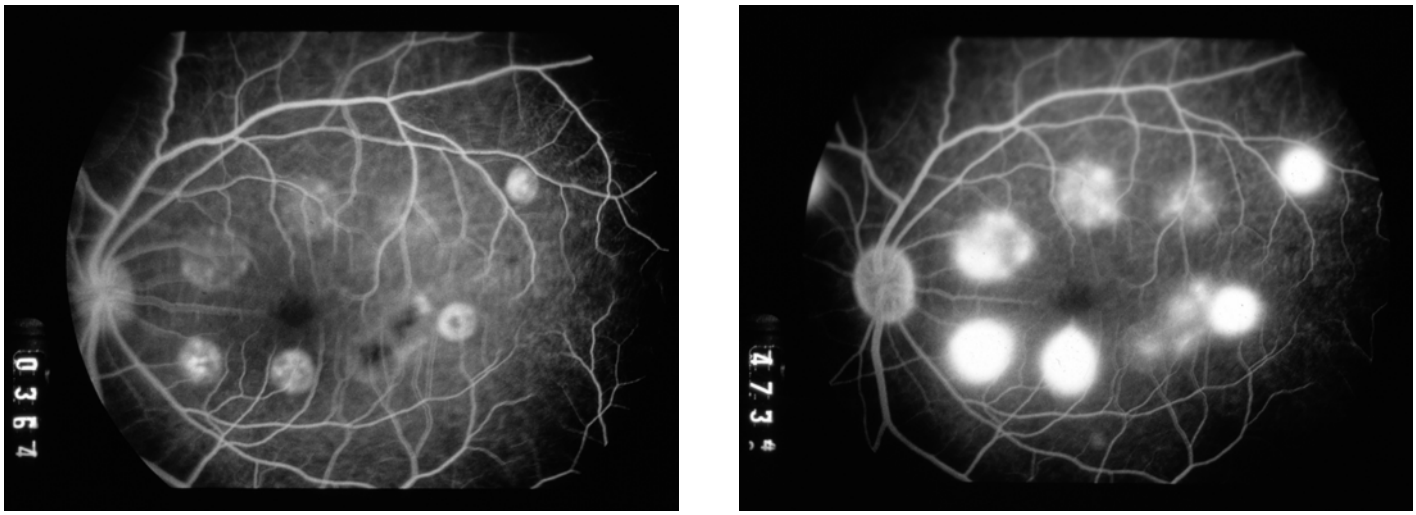

FIGURE 4

Fundus fluorescein angiogram during transit (left) and late in the angiogram (right) showing early hypofluorescence with late staining and leakage.

Histopathologic examination of PDT lesions (150 to 1800 mW/cm^2) revealed that the choriocapillaris was closed, packed with platelets and red blood cells, with vacuolated RPE and rare pyknotic nuclei in the outer nuclear layer (ONL) at all irradiances. Light microscopy of a lesion irradiated at 1200 mW/cm^2 is shown in Figure 6. Ultrastructural examination of PDT lesions irradiated at 150 to 1200 mW/cm^2 (Figures 7 and 8) showed endothelial cell damage in the choriocapillaris with platelet thrombus, vacuolation of the RPE, and loss of basal infoldings (Figure 7, right). Outer segments appeared infrequently damaged. There was no evidence of denatured collagen. In the lesion irradiated at 1800 mW/cm^2, there was increased collateral damage in the choroid (Figure 9), including vacuolated endothelial cell cytoplasm in the larger vessels and damage to the retinal vasculature and inner nuclear layer cells. Rare pkynotic nuclei were seen at light microscopy. There was no evidence of collagen denaturation. The PDT lesion using 1800 mW/cm^2 was irradiated 5 minutes after dye injection, which may have contributed to the retinal and choroidal vascular damage noted.

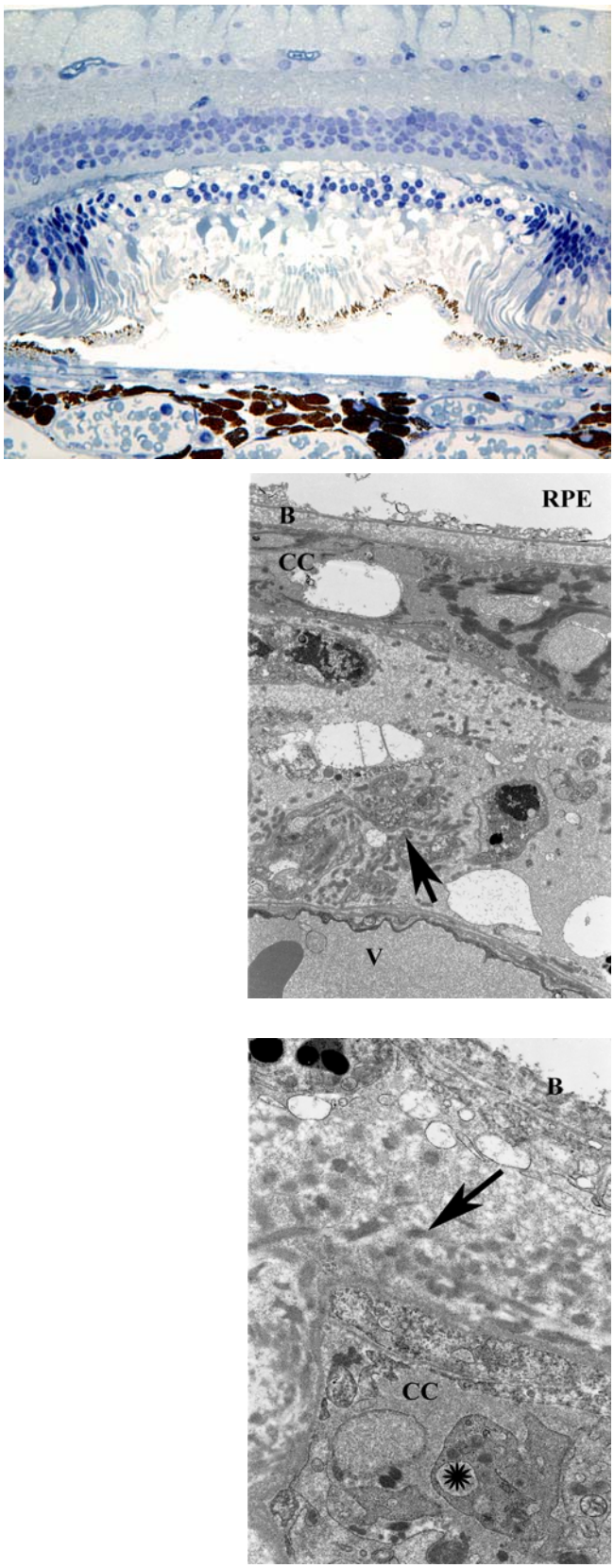

FIGURE 5

Top, After irradiation with 37,500 mW/cm^2 irradiance (lesion I, 692 nm with no dye), the outer retina is completely destroyed with no surviving receptor cells or retinal pigment epithelium (RPE) cells. Choriocapillaris shows evidence of thrombosis while larger choroidal vessels remain open. Denatured collagen is present but not visible at this magnification (toluidine blue, original magnification ×40). Middle, After irradiation at 37,500 mW/cm^2, the choroid below Bruch's membrane (B) shows the choriocapillaris (CC) closed, endothelium damaged, and fibrin present within the capillary. The retinal pigment epithelium above (RPE) is destroyed. Between the choriocapillaris and a larger vessel below (V) are damaged cells, large vacuoles, debris, plasma infiltrate, and fibrils of denatured collagen (arrow) (uranyl acetate and Sato's lead stain, original magnification ×3900). Bottom, Higher magnification of the area of lesion I shows fibrils of denatured collagen (arrow) around a choriocapillaris (CC) closed by platelets (asterisk) (uranyl acetate and Sato's lead stain, original magnification ×11,500). B, Bruch's membrane.

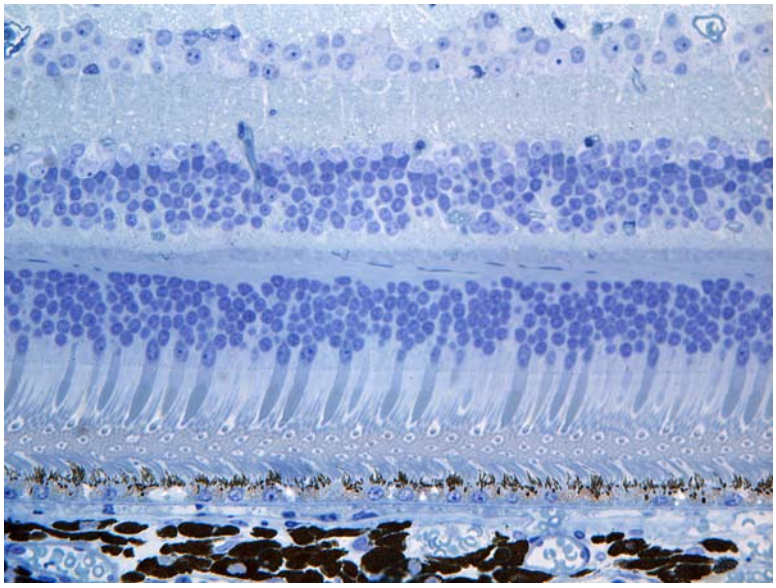

FIGURE 6

Retina appears normal in lesion L after irradiation with 1200 mW/cm^2 irradiance except for vacuolation of the retinal pigment epithelium (RPE) and platelet thrombi found in some choriocapillaris vessels. Rare pyknotic outer nuclear layer nuclei were seen and all larger choroidal vessels were patent (toluidine blue, original magnification ×40).

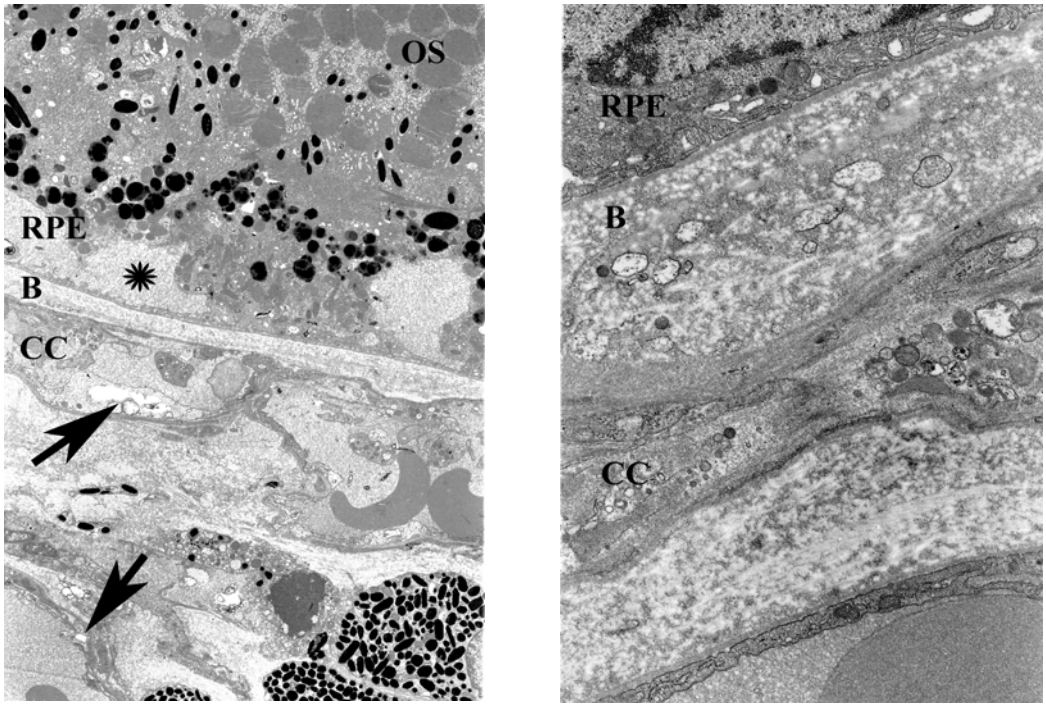

FIGURE 7

Left, In lesion M, an area of retina irradiated with 600 mW/cm^2 irradiance, the retinal pigment epithelium (RPE) appears damaged with large extracellular pools of electron dense material (asterisk) present. The choriocapillaris (CC) shows damage to the endothelium (arrow) and platelets in the lumen, and a larger vessel below shows vacuolation of the endothelium (arrow). The matrix appears edematous and a dying cell is seen, but no evidence of denatured collagen is noted. Outer segment (OS) profiles above the RPE appear infrequently damaged (uranyl acetate and Sato's lead stain, original magnification ×2200). Bruch's membrane (B). Right, Higher magnification of lesion M shows a surviving RPE cell (RPE) with vacuoles and a loss of basal infoldings, platelet-filled choriocapillaris (CC), and normal endothelium on a larger vessel below. There is increased edematous opacity to the matrix and some debris in Bruch's membrane (B) but no denatured collagen (uranyl acetate and Sato's lead stain, original magnification ×8900).

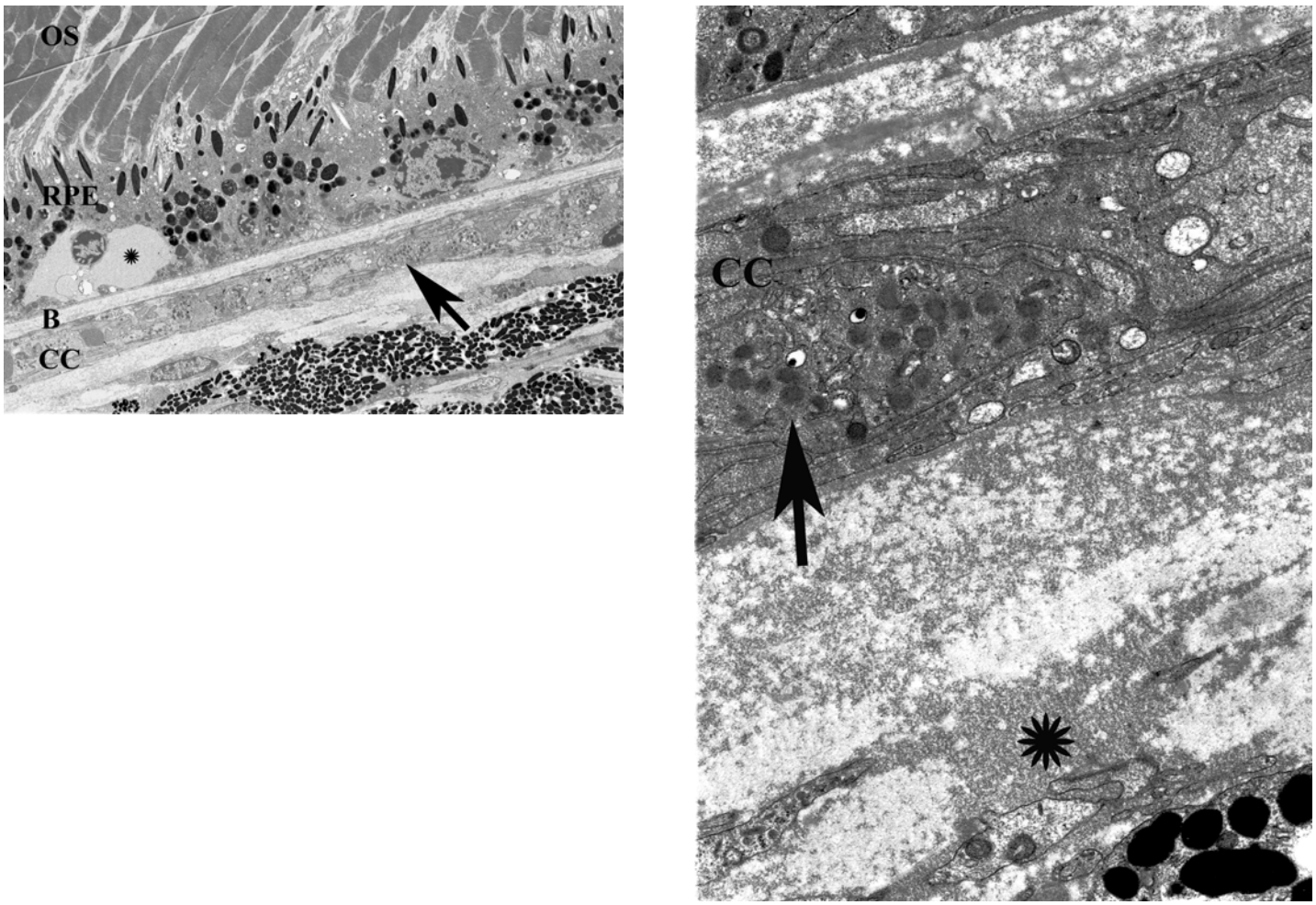

FIGURE 8

Left, Irradiation with 1200 mW in lesion L produces closure of the choriocapillaris (CC) with platelet thrombus (arrow), some damage to the retinal pigment epithelium (RPE) including cytoplasmic condensation and vacuolation (asterisk), and little change to the outer segments (OS). The matrix has some infiltrate, matrix cells show minimal changes, and there is no evidence of denatured collagen (uranyl acetate and Sato's lead stain, original magnification = ×1650). Bruch's membrane (B). Right, Higher magnification of the 1200-mW/cm^2 spot at lesion L shows the choriocapillaris (CC) closed by platelet thrombus (arrow), plasma infiltrate in the matrix (asterisk), and no evidence of denatured collagen. (uranyl acetate and Sato's lead stain, original magnification ×8900).

CONCLUSIONS

We tested PDT using verteporfin BPD-MA in normal eyes at irradiances of 150 to 1800 mW/cm^2 and found no evidence of thermal damage to collagen fibrils by electron microscopy at these doses (Moulton RS, ARVO Meeting, 1993, Abstract). Laser irradiation without dye produced clinically visible lesions at 37,500 mW/cm^2 with gross disruption of retinal structure and collagen denaturation. Laser photocoagulation of retina in the clinical setting is typically in the range of 100,000 to 1,000,000 mW/cm^2, orders of magnitude higher than the levels tested for PDT here. These data suggest that the effects of PDT using BPD-MA are primarily photochemical rather than thermal at irradiances as high as 1800 mW/cm^2, although at this irradiance mild damage to inner retina and large choroidal vessels was observed. It is worth noting that the 1800 mW/cm^2 lesion was made 5 minutes after the end of the dye infusion, and localization and angiography studies of BPD-MA in rabbit and monkey eyes have revealed that the BPD-MA level in the retinal and choroidal vessels and RPE is relatively high at this early timepoint.[86] These experiments demonstrated that irradiances higher than 200 mW/cm^2 could be used in PDT for CNV without the risk of producing a profound thermal effect. The mild hyperthermia that may be produced with higher irradiances may act synergistically with PDT to potentiate cell killing.[87]

These experiments provided the basis for proceeding with PDT of experimental CNV at higher irradiances. PDT of CNV using BPD-MA in DMSO was performed at irradiances of 300 and 600 mW/cm^2 and showed effective closure of CNV (J. W. Miller, MD, unpublished data).[7] These parameters were well within the range for nonthermal damage and provided much shortened treatment

times, and 600 mW/cm^2 was selected for development of a clinical therapy.[7,88] Treatment parameters were further explored with verteporfin (BPD in liposomal formulation), and much of this work has been published.[6,8-11] Interestingly, investigations of PDT for AMD using other photosensitizers have adopted the higher irradiance of 600 mW/cm^2 as the standard irradiance parameter (Baumal C, ARVO Meeting, 1996, Abstract; Arbour J, ARVO Meeting, 1999, Abstract).

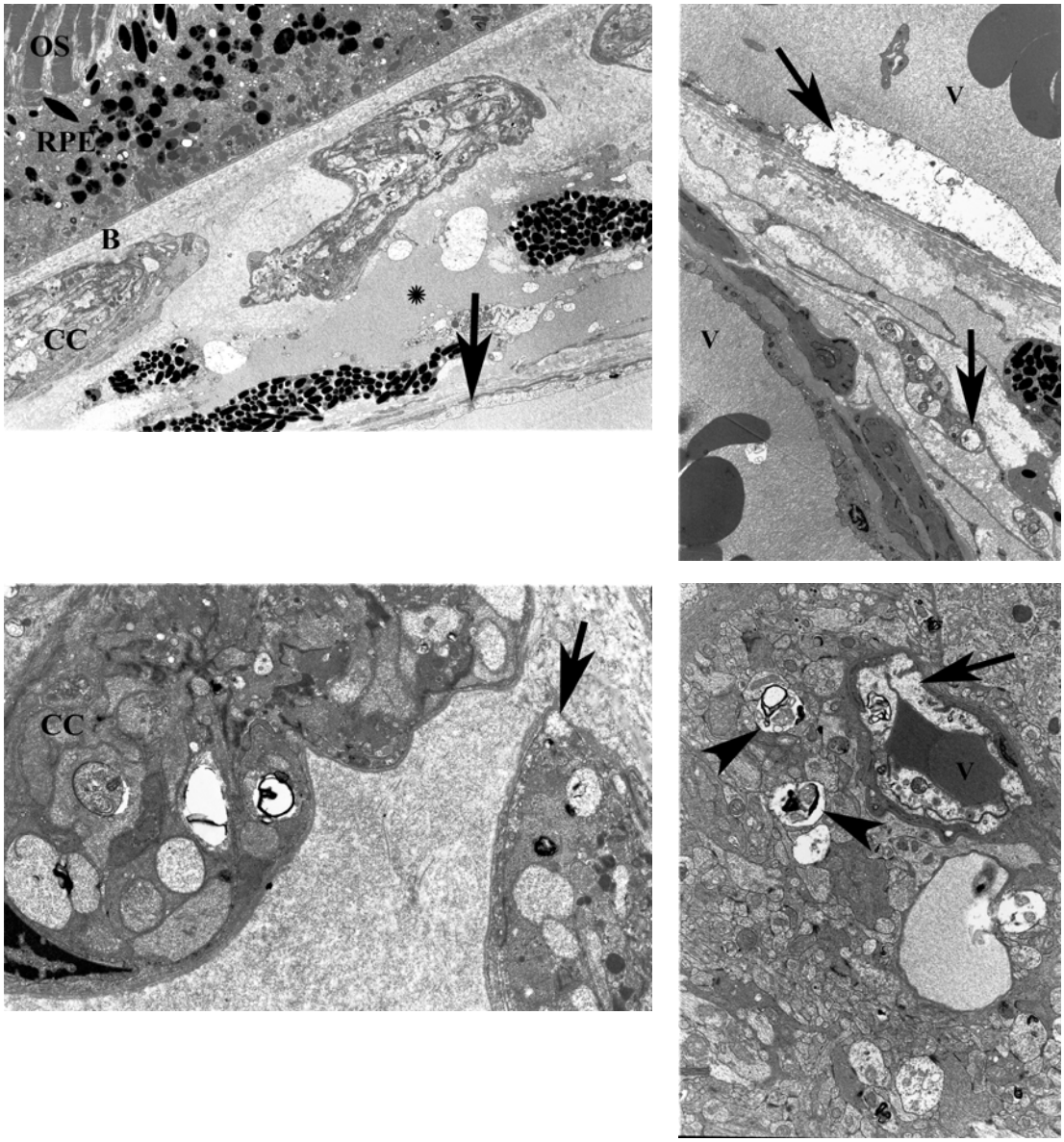

FIGURE 9

Top left, In lesion K, the area of retina irradiated with 1800mW/cm^2 with dye, outer segments (OS) appear normal, while the RPE (RPE) shows some vacuolation and loss of basal infoldings. The choriocapillaris (CC) is closed by platelet thrombus. The matrix shows plasma infiltration (asterisk) and damaged cells with debris. A larger vessel at the bottom shows endothelial disruption (arrow). No evidence of collagen denaturation. (uranyl acetate and Sato's lead stain, original magnification ×2200). Bruch's membrane (B). Top right, In lesion K, deeper choroidal vessels (V) show damage to the endothelium (arrow) and vacuolation to matrix cells (arrow), but no denatured collagen is seen (uranyl acetate and Sato's lead stain, original magnification ×2950). Lower left, Higher magnification of lesion K shows closure of two choriocapillaries (CC) by platelets and fibrin with endothelial damage (arrow). The matrix shows normal collagen. (uranyl acetate and Sato's lead stain, original magnification ×6610). Lower right, Retinal vessels are affected at 1800 mW/cm^2 irradiance. This capillary (V) in lesion K shows damaged endothelium (arrow) and some of the surrounding nerve fibers are also affected (arrowheads) (uranyl acetate and Sato's lead stain, original magnification ×5200).

OVERVIEW OF THE DEVELOPMENT OF VERTEPORFIN PDT

In the preclinical studies of verteporfin PDT, both BPD-MA dissolved in DMSO and liposomal BPD, or verteporfin, were tested. Doses ranging from 0.25 to 2 mg/kg of verteporfin, fluence rates of 50 to 600 J/cm^2, and irradiances of 150 to 1800 mW/cm^2 were investigated, and details of the treatments are provided elsewhere.[7-9] Laser irradiation was performed earlier after drug injection than in the tumor models, as it was hypothesized that this would be more effective in treating neovasculature. Overall, in the development of PDT, 55 cynomolgus monkeys were used in experiments (8 in experiments using BPD-LDL on normal choroid and CNV including high irradiance, and 47 in experiments using the liposomal formulation, or verteporfin. Of the animals used in experiments of verteporfin, 19 animals were used in dye dose ranging studies, with 4 animals followed for 4 to 7 weeks to determine the long-term changes. Additionally, variable irradiance and fluence were tested in 7 animals, 3 in CNV and 4 in normal choroid; 14 animals were used to evaluate variable infusion times; and 7 animals were used to test for the effects of multiple treatments on normal choroid). PDT using both BPD-MA in DMSO and verteporfin led to effective closure of CNV, evidenced by absence of angiographic leakage from CNV 24 hours after treatment, with a wide range of treatment parameters. Histologically, PDT-treated CNV demonstrated thrombosis of vessels within the CNV, with closure of choriocapillaris and necrotic RPE. In general, decreasing the verteporfin dose led to a narrower time window in which laser irradiation would produce CNV closure. At a verteporfin dose of 0.375 mg/kg, or approximately 6 mg/m^2, effective occlusion of CNV could be achieved if irradiation with 690-nm laser light was performed within 50 minutes of verteporfin infusion.

Since the laser injury model necessarily showed damage to the outer retina secondary to the thermal laser injury, the selectivity of PDT in normal eyes was investigated. A histologic grading scheme based on damage to the ONL, damage to retinal vessels and large choroidal vessels, and neurosensory retina was developed (Table 5).[8] Unacceptable damage was defined as any of the following: pyknosis of the ONL >50%, damage to retinal vessels, or damage to large choroidal vessels. Acceptable damage was pyknosis of the ONL to a lesser degree, mild disruption of the outer segments, choriocapillaris occlusion, and RPE necrosis. Overall, decreasing verteporfin doses led to less damage.[8,9] At a verteporfin dose of 0.375 mg/kg, irradiation at 20 minutes or longer after the start of verteporfin infusion typically led to closure of choriocapillaris and RPE necrosis, with pyknosis in the ONL of ≤50%, and no damage to retinal or large choroidal vessels, ie, grade 3 or less. Irradiation within 10 minutes of the start of verteporfin infusion at a variety of doses caused damage of retinal vessels, or grade 5, and was deemed unacceptable.

TABLE 5. GRADING SCHEME OF PHOTODYNAMIC THERAPY EFFECT ON RETINA AND CHOROID

GRADE	DAMAGED RETINAL/CHOROIDAL LAYERS
1	RPE only or RPE + slight photoreceptor changes + occasional pyknosis in the ONL; with or without choriocapillaris damage
2	Choriocapillaris closure + RPE + photoreceptors + 10%-20% pyknosis in the ONL
3	Choriocapillaris closure + RPE + photoreceptors + ONL pyknosis <50%
4	Choriocapillaris closure + RPE + photoreceptors + ONL pyknosis >50%
5	Choriocapillaris closure + RPE + photoreceptors + ONL pyknosis >50% + choroidal vessel damage or retinal vessel or inner retinal damage

ONL, outer nuclear layer; RPE, retinal pigment epithelium.
Adapted from Kramer M et al.[8]

We investigated PDT performed at higher irradiances in normal eyes and CNV (as described in more detail above) and demonstrated that irradiances higher than those typically used in dermatology (<200 mW/cm^2) were safe and effective for the treatment of CNV and greatly improved the practical application of PDT in ophthalmology. As described above, PDT of normal choroid showed no thermal damage, as evidenced by collagen fibril structure on electron microscopy, at irradiances as high as 1800 mW/cm^2 (Moulton RS, ARVO Meeting, 1993, Abstract). Furthermore, PDT of normal choroid using BPD in DMSO (1 mg/kg) at irradiances of 300 and 600 mW/cm^2 examined at 24 hours showed grade 1 and 2 damage, with RPE necrosis, closure of choriocapillaris but preserved retinal and larger choroidal vessels, and 10% to 20% pyknosis of the ONL (J.W. Miller, MD,

unpublished data). PDT of CNV using BPD in DMSO at irradiances of 300 and 600 mW/cm^2 was effective in closing experimental CNV.[7] Additional studies showed that CNV closure could be obtained at higher irradiances up to 1200 mW/cm^2 (J. W. Miller, MD, unpublished data). Together, this data supported the safety and efficacy of higher irradiance for PDT of CNV.

As noted above, a series of experiments using liposomal BPD (or verteporfin) identified an optimal dye dose (0.375 mg/kg or 6 mg/m^2) and time of irradiation after dye injection (between 20 and 50 minutes) and have been described in published papers [8,11] with irradiance and fluence fixed at 600 mW/cm^2 and 150 J/cm^2. Further studies were carried out using liposomal BPD or verteporfin, varying irradiance (Table 6) and fluence (Table 7) in experimental CNV and normal choroid (J. W. Miller, MD, unpublished data). In the irradiance experiments, one animal was used for CNV and 1 animal for normal choroid, using a dye dose of 0.375 mg/kg, 150 J/cm^2, and varying irradiance: 150, 300, 600, 900, 1200, 1500, and 1800 mW/cm^2. Eight CNVs in one monkey were treated using variable irradiances, and all showed angiographic and histologic closure of CNV vessels with irradiances of 150, 300, 600, and 900 mW/cm^2. The lesion treated with 1200 mW/cm^2 showed some hemorrhage in the choroid and open vessels in the CNV. This lesion was irradiated at 52 minutes after dye injection and may have been beyond the time threshold for PDT effect. PDT of normal choroid at varying irradiances was also investigated. Ten areas of normal choroid in one monkey were treated with PDT using irradiances from 300 to 1800 MW/cm^2. These areas were assessed angiographically at 24 hours and then graded histologically using the histologic grading scheme developed and published by our group[8] (Table 5). This evaluation was made using light microscopy only and did not examine thermal damage of collagen fibrils. At 300 mW/cm^2, one area showed grade 1 damage and one area showed grade 4 damage. At 600 mW/cm^2, one area had grade 3 damage and one area had grade 5 damage with closure of medium-sized choroidal vessels. At 900 mW/cm^2, one area had grade 3 damage, and one area had grade 5 damage. Both areas had grade 5 damage at 1200 mW/cm^2. At 1500 mW/cm^2, the area treated had grade 5 damage. At 1800 mW/cm^2, the one treated area had grade 3 damage with the time of irradiation 56 minutes after BPD infusion. We had decided that grades 4 and 5 represented unacceptable damage to surrounding structures, characterized by either damage to normal retinal vessels or to larger choroidal vessels or demonstrating greater than 50% pyknosis of photoreceptor nuclei. Therefore, PDT using liposomal BPD at 0.375 mg/kg and fluence of 150 J/cm^2 with irradiance of 1200 mW/cm^2 and higher seemed to cause unacceptable damage, although the number of areas tested were relatively few. Irradiance of 600 mW/cm^2 showed significant damage in one lesion out of two but was further tested extensively in additional animals[8] and found to be safe, causing mild photoreceptor pyknosis. Treatment using 900 mW/cm^2 may be problematic. The observed damage, in part, was likely a direct PDT effect on retinal and choroidal vessels. Pyknosis of photoreceptors, indicating apoptosis, could be a direct PDT effect on photoreceptors, but was more likely due to inflammation-mediated damage as described more recently by our group.[51] These high-irradiance results extend and qualify the initial feasibility experiment described in this manuscript that looked for collagen denaturation as a marker of thermal damage. Interestingly, varying the irradiance did not appear to affect closure of CNV.

TABLE 6. VARIABLE IRRADIANCE PARAMETERS AND EFFECTS ON NORMAL CHOROID AND CHOROIDAL NEOVASCULARIZATION (CNV) USING LIPOSOMAL BPD (OR VERTEPORFIN)

	NORMAL CHOROID		CNV		
IRRADIANCE (mW/cm^2)	**TIME* OF IRRADIATION (MIN)**	**CHOROID GRADE**	**TIME* OF IRRADIATION (MIN)**	**NUMBER OF CNV CLOSED**	**NUMBER OF CNV LESIONS**
150	Not done		15, 62	2	2
300	16, 51	1, 4	20, 36	2	2
600	27, 37	3, 5	34	1	1
900	27, 38	5, 3	42, 51	2	2
1200	21, 46	5, 5	52	0	1
1500	15	5	Not done		
1800	56	3	Not done		

*Number of minutes at which light was applied after dye infusion.

Experiments in which fluence was varied were also undertaken to establish a therapeutic window at a fixed dye dose of 0.375 mg/kg and fixed irradiance of 600 mW/cm^2. Two animals were used for CNV and 2 for normal choroid with the following fluences: 50, 100, 200, 400, and 600 J/cm^2. Ten CNVs in 2 monkeys were treated with variable fluences. At 50, 100, and 200 J/cm^2, half (3 of 6) of the CNVs were closed. At 400 and 600 J/cm^2, all CNVs were closed, but in one of each of the CNVs treated with 400 or 600 J/cm^2, an overlying serous retinal detachment was evident clinically and histologically following treatment. Two normal monkeys were treated with variable fluences, but only one was examined histologically and graded using the grading scheme described above. A total of 15 treated areas were examined. At 50 and 100 J/cm^2, the angiogram 24 hours after PDT showed faint staining and

histopathology showed grade 1 damage with open choriocapillaris. At 200 and 600 J/cm^2, there was grade 1 damage. At 400 J/cm^2 there was grade 2 damage. Variable fluence data in the normal choroid suggested that no great difference in effect was seen at fluences ranging from 50 to 600 J/cm^2. In contrast, when CNVs were treated, a serous retinal detachment was noted when fluences of 400 and 600 J/cm^2 were utilized, suggesting an upper limit of safety below 400 J/cm^2. The greater effect noted in CNV may be related to PDT effect on resident macrophages in areas of CNV, as suggested more recently by the work of our group.[51]

TABLE 7. VARIABLE FLUENCE PARAMETERS AND EFFECTS ON NORMAL CHOROID AND CHOROIDAL NEOVASCULARIZATION (CNV) USING LIPOSOMAL BPD (OR VERTEPORFIN)

	NORMAL CHOROID		CNV			
FLUENCE (J/cm^2)	**TIME* OF IRRADIATION (min)**	**CHOROID GRADE**	**TIME* OF IRRADIATION (min)**	**NUMBER OF CNV LESIONS**	**NUMBER OF CNV CLOSED (time* in min)**	**ADVERSE EFFECTS (time* in min)**
50	20,† 20, 42	1	20, 45	2	1 (20)	
100	25, 32,† 46	1	24, 64	2	1 (24)	
200	40,† 50, 73	1	31, 37	2	1 (31)	
400	50,† 54, 70	2	20, 39	2	2	Small serous RD (39)
600	22, 29, 60†	1	47, 53	2	2	Large serous RD (53)

RD, retinal detachment.
*Number of minutes at which light was applied after dye infusion.
†Treated areas examined histologically. Others could not be examined as the eye was too distorted following enucleation and fixation. Angiographic examination of these other lesions at 24 hours showed no effect in the treated areas or faint staining or noticeable staining of the areas in the late frames of the angiogram. No serous retinal detachment was noted in treated areas of normal choroid.

Although there was no safety concern using a bolus verteporfin injection from the nonhuman primate studies, liposomal drugs are typically used clinically as an intravenous infusion, and the clinical trials of verteporfin PDT in dermatology used a 30-minute intravenous infusion. Further studies were undertaken in the monkey to evaluate the safety and efficacy of PDT using an intravenous infusion of verteporfin.[9] Following a 10-minute intravenous infusion, effective closure was achieved when irradiation was performed 20 to 30 minutes after the start of infusion using a spot size of 1250 to 3000 μm, 689-nm light at 600 mW/cm^2 and 150 J/cm^2.[9]

Studies were performed to examine the longer-term effects of PDT using verteporfin on the treated CNV as well as normal retina and choroid.[11] Persistent closure of CNV (out to 4 weeks) was seen in eyes that had been treated with the optimal parameters, and histopathology demonstrated a fibrous scar covered by proliferating RPE, with few open capillaries. In normal eyes treated with PDT, the choriocapillaris was reperfused by 4 weeks, and the RPE appeared to be repopulated with variable pigmentation. Pigmented macrophages were noted overlying the RPE, and there was mild disorganization of the photoreceptor outer segments. It appeared that the damage to the RPE and choriocapillaris noted acutely recovered by 4 to 7 weeks.

Since early clinical studies suggested that PDT might need to be repeated, studies were undertaken to assess the recovery following multiple PDT treatments of normal eyes.[6] Three sequential PDT treatments were performed in the same area of normal retina and choroid. Three doses of liposomal BPD were studied (6, 12, and 18 mg/m^2) with the light doses kept constant (689 nm, 600 mW/cm^2, 100 J/cm^2). Treatments were separated by 2 weeks, and histopathologic examination was performed at 2 and 6 weeks after the third treatment. Minimal damage was seen in the group treated at 6 mg/m^2, with recovery comparable to the single treatment at 0.375 mg/kg (approximately 6 mg/m^2). However, higher dye doses led to significant cumulative damage to the normal retina, choroid, and optic nerve, emphasizing that selectivity of PDT with verteporfin is relative and dose-dependent.

The experiments underlying the development of verteporfin PDT for clinical application were in large part empiric, rather than mechanistic, but additional studies were undertaken to elucidate the tissue effects following PDT of CNV. In the cancer literature, PDT using verteporfin had been demonstrated to catalyze the formation of reactive oxygen intermediates and to rapidly induce apoptosis in a variety of cell types after light irradiation.[6-10,50] Using another photosensitizer, lutetium texaphyrin, we found that PDT in vitro causes apoptosis of retinal capillary endothelial cells and RPE, with caspase-3 activation.[11,50,89] Generally, the activation of caspases, a family of cysteine proteases, is a central event in apoptosis, although caspase-independent apoptosis also occurs in some systems.[36,51] To investigate mechanisms of apoptosis after PDT of CNV in vivo, we first translated the primate verteporfin angiography and PDT methodology to the rat.[90] Using TUNEL staining as a marker of apoptosis, we found that while CNV did not

show apoptosis prior to PDT, TUNEL-positive cells could be recognized as early as 1 hour after PDT, increasing at 3 hours, peaking at 6 hours, and then decreasing at 48 hours, showing a dose-dependence with respect to verteporfin dose. Cleaved caspase-3 and cleaved caspase-9 followed a similar but earlier course, peaking at 3 hours and decreasing by 24 hours after PDT, suggesting caspase activation early after PDT in endothelial cells of CNV, preceding TUNEL positivity. We also investigated the role of Akt in endothelial cell survival after PDT. A serine/threonine kinase, Akt/protein kinase B is a downstream effector of phosphatidylinositol-3 kinase (P13K), an important regulator of endothelial cell survival downstream of VEGF. Phosphorylated Akt (pAkt) promotes cell survival by inhibiting apoptotic signals such as caspase-9, Bad, and others. We found that prior to PDT, nearly all cells in CNV were positive for pAkt with no TUNEL positivity, but within 1 hour after PDT the number of pAkt-positive cells was significantly reduced, and that this was an effect of phosphorylation, since the Akt protein level was not reduced. The results suggest that dephosphorylation of Akt precedes apoptotic cell death in CNV. Interestingly, while Akt phosphorylation remained suppressed by PDT for 24 hours, pAKT-positive cells returned to baseline by 48 hours and may contribute to cell survival and CNV recurrence.

To investigate the role of inflammation in CNV after PDT, we studied expressional changes of inflammatory cytokines and recruitment of inflammatory cells after PDT.[91] We demonstrated significant increases in mRNA for MCP-1 and IL-1B 24 hours after PDT, whereas other cytokines, including CCR2 (MCP-1 receptor), did not change. We also observed that the number of neutrophils in CNV increased following PDT, and it is possible that MCP-1 causes this neutrophil recruitment.[91]

While PDT-induced apoptosis in CNV is a requirement for efficacy of therapy, we have also observed photoreceptor apoptosis after PDT in monkey and rat models, which is an unwanted toxicity.[51] PDT causes direct cytotoxicity via singlet oxygen and reactive oxygen intermediates, but these are extremely short-lived, and direct damage necessitates photosensitizer contact with the cell. While photosensitizer may reach the photoreceptors via diffusion, this is not likely to be significant. However, PDT may also cause indirect damage to the tissue via effects on inflammatory cells in tissue undergoing treatment; these cells may be activated by PDT and secondarily lead to photoreceptor damage. In monkey and rat eyes with laser-induced CNV, TUNEL-positive cells were detected in the photoreceptor layer at 6 and 24 hours after PDT, but unlike CNV cells, photoreceptor TUNEL staining was greater at 24 hours.[51] TUNEL-positive cells were not noted in regions not exposed to light for PDT. Cleaved caspase-3 was noted in CNV after PDT, as previously described, but was not evident in the retina. Using ED-1, a macrophage marker, we looked for migration of macrophages following PDT, but although macrophages were found localized to the laser-injured retina, there was no increase in the number of macrophages following PDT. Although macrophages did not appear to be increased after PDT, we were still suspicious that macophages were playing a role in photoreceptor degeneration, since the TUNEL-positive photoreceptors were noted near the sites of original laser injury where macrophages were also found. Indeed, we demonstrated that iNOS was increased in macrophages and that NOS inhibition reduced photoreceptor apoptosis following PDT. In follow-up studies, we found that intraperitoneal dexamethasone 1 hour before PDT reduced the number of TUNEL-positive cells in the photoreceptor layer. It is possible that the clinical observation that PDT combined with intravitreal corticosteroid may lead to better vision outcomes results from the corticosteroid inhibition of this macrophage activation and photoreceptor apoptosis. Interestingly, NOS inhibition did not interfere with CNV closure following PDT in the rat model, and intraperitoneal dexamethasone given prior to PDT actually increased CNV closure rates.[51,91]

The cellular events following PDT of CNV, involving inflammatory cytokines, cells, photoreceptors, and RPE, are complicated, and likely both drug and light dose-dependent. Both desired and unwanted effects may result from indirect action on bystander cells and pathways. However, these pathways also offer opportunity to manipulate the therapeutic effects to optimize CNV closure and minimize photoreceptor apoptosis. Further studies are warranted.

BPD ANGIOGRAPHY IN NONHUMAN PRIMATES AND PATIENTS

Angiography using verteporfin was first investigated as a means of confirming the timing of localization of the photosensitizer to the neovascular tissue. However, its spectral characteristics, with an absorption/excitation spectrum between 350 and 690 nm (with absorption maxima at 354, 418, 574, 626, and 688 nm),[92,93] and fluorescence emission in a narrow band with maximum at 690 nm,[93] suggested that it might be a useful dye for angiography of choriocapillaris and CNV (Figure 10). Verteporfin fundus angiography of experimental CNV using a modified fundus camera and digital imaging system, with a pair of matched interference filters consisting of an excitor filter centered at 580 nm (halfwidth: 60 nm) and a barrier filter centered at 696 nm (halfwidth: 50 nm), was performed (Kramer M, ARVO Meeting, 1995, Abstract).[94] In the same eyes, fluorescein angiography and indocyanine green angiography were also performed. Verteporfin angiography provided clear imaging of the small choroidal vessels, and areas of CNV showed early hyperfluorescence (9 to 14 seconds), delineation of the CNV (5 to 30 minutes), and mild leakage later in the study (starting at 30 to 50 minutes) (Figure 11). When clinical trials were initiated, verteporfin angiography was also carried out in several patients. However, because verteporfin was administered as an intravenous infusion rather than a bolus injection, the images were not as high-quality (Figure 12). It is possible that further refinements could enhance the contrast and improve the technology.

CLINICAL TRIALS OF VERTEPORFIN PDT

Based on the experimental studies in nonhuman primates, Phase 1/2 clinical studies were initiated with the first patient treated at Massachusetts Eye and Ear Infirmary in 1995. Sixty-one patients with subfoveal CNV containing some classic CNV secondary to AMD and other disorders were enrolled in a safety and dose-ranging trial (Schmidt-Erfurth U, ARVO Meeting, 1996, Abstract; Miller JW, ARVO Meeting, 1996, Abstract).[95] Verteporfin doses were 6 or 12 mg/m^2 infused over 10 or 5 minutes with laser light of 689 nm applied 10, 15, 20, or 30 minutes after the start of infusion with a fluence of 50 to 150 J/cm^2 and an irradiance of 600 mW/cm^2. A maximum tolerated fluence was identified as retinal vessel occlusion was noted at 150 J/cm^2, and a minimal effective dose with

inconsistent CNV closure at 25 J/cm^2. Overall, verteporfin PDT led to cessation of angiographic leakage from CNV evident at 1 to 4 weeks after treatment, but by 12 weeks, leakage recurred in most cases. Other than the ocular side effects noted above, verteporfin PDT was well tolerated. Based on these results, a Phase 3 trial, Treatment of Age-related Macular Degeneration using Photodynamic Therapy (TAP) Trial, was undertaken using 6 mg/m^2 infused over 10 minutes with light irradiation 15 minutes after the start of drug infusion, using 50 J/cm^2 and 600 mW/cm^2.[96] Eligible patients had subfoveal CNV secondary to AMD with a classic component, refracted vision of 20/40 to 20/200, and a lesion size of 5400 μm or less. Patients were randomized 2:1 to verteporfin PDT or sham PDT and underwent retreatment every 3 months if fluorescein angiography demonstrated leakage. At 12 months of follow-up, 246 of 402 eyes (61%) lost fewer than 3 lines of vision from baseline compared to 96 of 207 eyes (46%) ($P < .001$). In subgroup analyses, the visual acuity benefit was clearly demonstrated in those with predominantly classic CNV, especially when there was no occult CNV. Few ocular or systemic adverse events were noted; events included transient vision disturbances, transient photosensitivity, vision decrease secondary to treatment, and infusion-related back pain. Two-year follow-up demonstrated that the beneficial outcomes of verteporfin were maintained.[97] One- and 2-year results showed no benefit to treatment for lesions that were minimally classic.

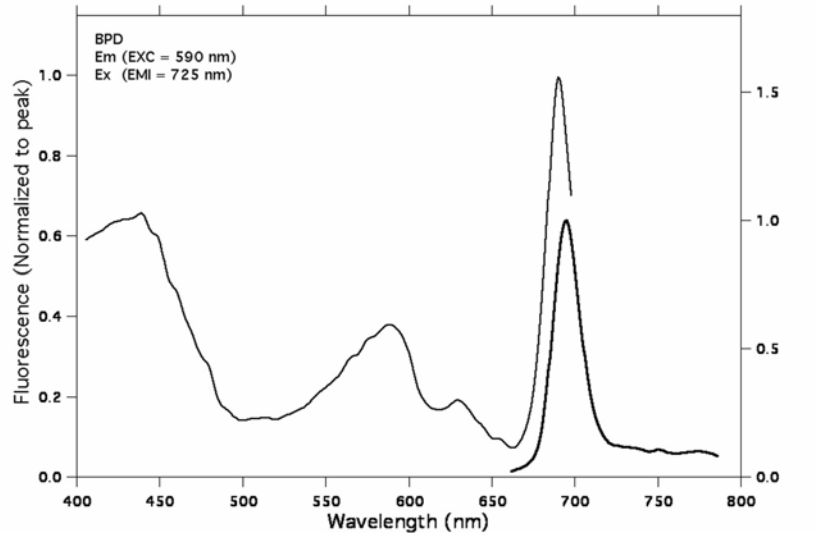

FIGURE 10

Absorption and fluorescence spectra for benzoporphyrin derivative (BPD).

The efficacy of verteporfin PDT for subfoveal CNV with occult but no classic angiographic components was further studied in the Verteporfin in Photodynamic Therapy (VIP) Study, enrolling 339 subjects in a multicenter, placebo-controlled, double-masked trial over 2 years.[98] While no difference was found at 1 year, treatment led to a decrease in the risk of moderate or severe vision loss at 2 years. Subgroup analysis showed a greater benefit in subjects with smaller (<4 disc areas) lesions and lower levels of visual acuity (20/50 or less). A meta-analysis of the VIP and TAP trials demonstrated that vision benefit correlated with smaller lesion size.[99] Subjects with CNV secondary to pathologic myopia were also studied in the VIP study and showed a benefit of verteporfin PDT at 1 and 2 years follow-up, confirming earlier results.[100] Another study of verteporfin PDT for occult CNV, the Verteporfin in Occult CNV (VIO) trial did not reach its primary end point (www.qltinc.com, 2005 press release), raising some additional doubt regarding the efficacy of PDT for occult lesions.

An additional clinical trial, the Verteporfin in Minimally Classic CNV (VIM) Study, was designed to compare the safety and efficacy of verteporfin PDT using standard laser parameters compared to altered laser parameters.[101] Although the trial emphasized the reduced fluence rate, both irradiance and fluence were reduced to 300 mW/cm^2 and 25 J/cm^2, respectively. Only patients with subfoveal CNV that was minimally classic with a lesion size ≤6 disc areas were eligible for enrollment. The study was able to demonstrate a treatment benefit of verteporfin overall (if the groups were combined), but the study was unable to demonstrate a benefit of the reduced fluence and irradiance parameters. Some of the problems with the study include: minimally classic CNV seems least responsive to verteporfin PDT in all studies; lesions in this study were larger than the small lesions shown in other studies to be more responsive; although the investigators were interested in studying reduced irradiance, fluence was reduced as well to a level (25 J/cm^2) shown to be of dubious benefit in the Phase 1 and 2 studies.[88]

Verteporfin PDT was shown to be of some benefit for patients with CNV secondary to other causes, including presumed ocular histoplasmosis syndrome (POHS), angioid streaks, inflammatory choroidopathies, idiopathic CNV, and others.[100,102-105]

FUTURE DIRECTIONS

Verteporfin PDT was the first pharmacologic therapy demonstrated to limit vision loss in patients with neovascular AMD and CNV secondary to other etiologies. Subsequently, other photosensitizers were investigated in animal models and clinical trials and utilized the higher irradiance parameter developed in the verteporfin experiments described above. However, none of these photosensitizers has proceeded through clinical trials to clinical application. More recently, antiangiogenic therapies have been developed and shown to benefit patients with neovascular AMD. In particular, 90% of patients treated with ranibizumab avoid moderate vision loss, and a remarkable one-third of patients show substantial vision improvement.[106] Monthly intravitreal injections are problematic for patients and physicians, and it remains to be seen to what extent PDT and other therapies may be combined with ranibizumab.

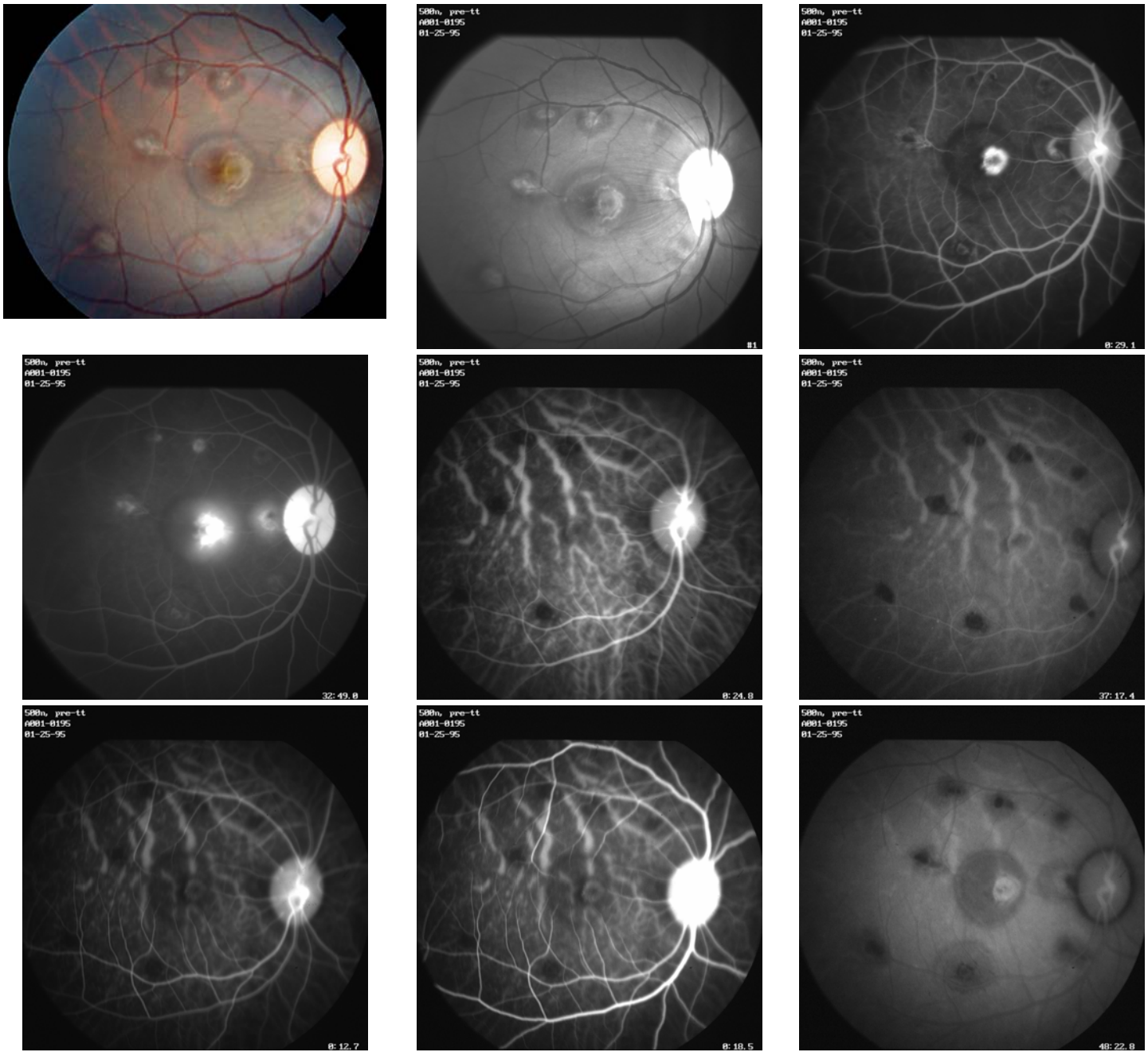

FIGURE 11

Benzoporphyrin derivative (BPD) angiography of experimental choroidal neovascularization (CNV). Fundus photography and angiography of experimental CNV in the nonhuman primate. Color image (top left) and red-free (top middle) photographs show pigment change in several areas corresponding to the laser injury sites and subsequent CNV. In the subfoveal region there is pigmented subfoveal tissue with elevation from subretinal fluid. Fluorescein angiography shows early hyperfluorescence (top right) at 29 seconds with late leakage (middle left) at 32 minutes from subfoveal CNV. Leakage from other areas of CNV are also apparent. Indocyanine green (ICG) angiography shows large choroidal vessels and retinal vessels; in the subfoveal area there is a web of early hyperfluorescence (middle center) at 24.8 seconds suggesting CNV, but without hot spots or plaques noted in the late frames (middle right) at 37 minutes. BPD angiography shows small choroidal vessels, retinal vessels, and early hyperfluorescence in the area of subfoveal CNV as early as 12 seconds (lower left) with clearer delineation of subfoveal CNV as a hyperfluorescent net (lower middle) at 18 seconds with persistent hyperfluorescence in CNV in later frames (lower right) at 48 minutes without leakage. Surrounding the CNV is a circular area of hypofluorescence corresponding to the area of subretinal fluid. BPD is no longer visible in most of the choroidal vessels or in the retinal vessels. (Reprinted with permission from Husain D et al.[94])

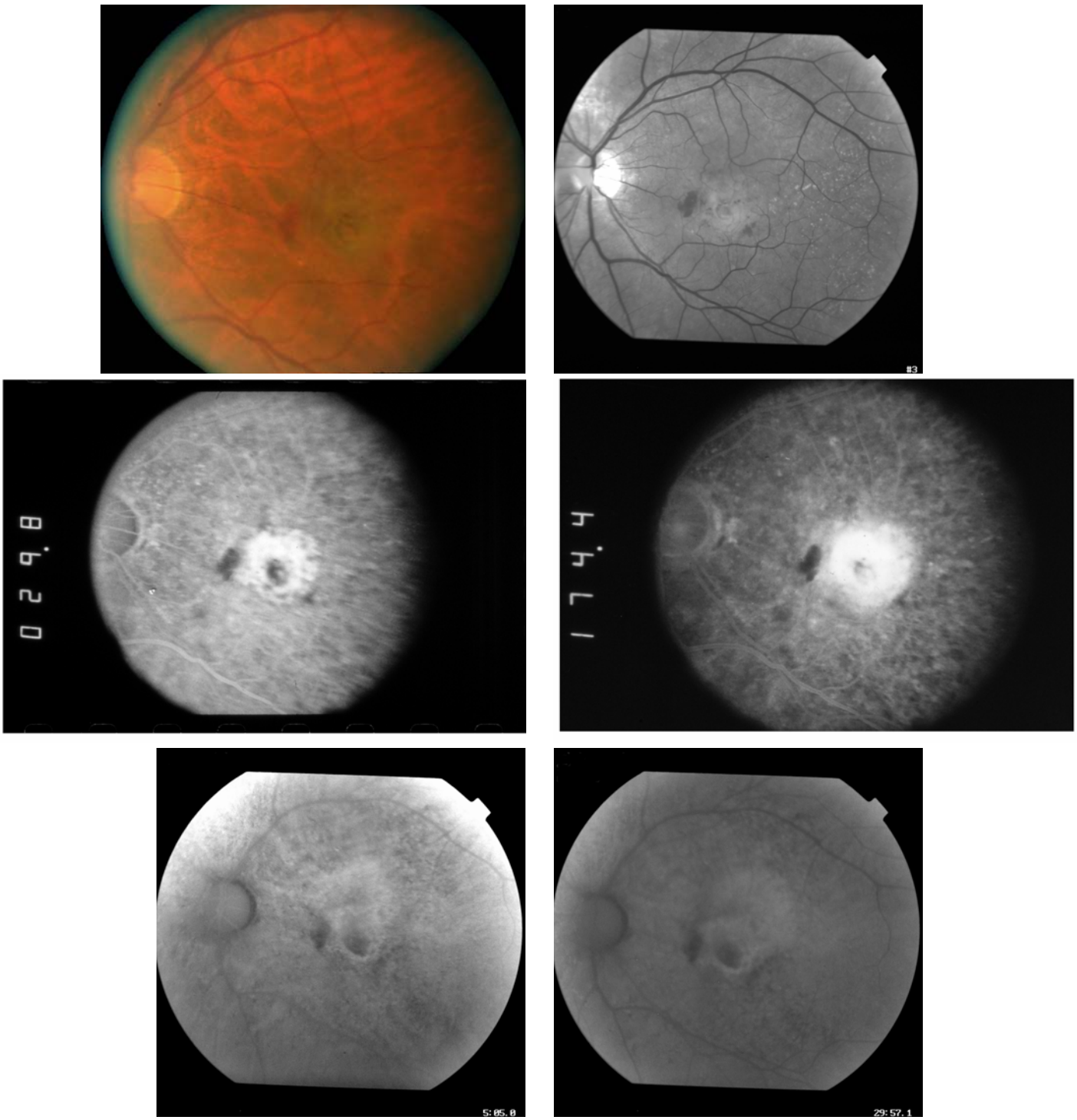

FIGURE 12

Benzoporphyrin derivative (BPD) angiography in patients with subfoveal choroidal neovascularization (CNV). Color (top left) and red-free (top right) photographs demonstrate subretinal tissue, hemorrhage, and fluid. Fluorescein angiography shows early hyperfluorescence (middle left) and late leakage (middle right) consistent with classic CNV. BPD angiography shows hyperfluorescence corresponding to the subretinal tissue at 5 minutes (lower left) with some fluorescence noted in retinal vessels overlying the disc; the hyperfluorescence of the subretinal tissue persists at 37 minutes (lower right).

Spaide and colleagues[56] first reported on combining intravitreal triamcinolone and PDT for neovascular AMD, describing improved visual acuity results and decreased frequency of retreatment. As noted above, there may be a biologic basis for improved

results from PDT combined with corticosteroids.[91] Additional series confirmed the results, although numbers of patients and follow-up were limited.[107] Spaide and colleagues[108] have also published on the use of PDT and intravitreal corticosteroids for nonsubfoveal lesions. Elevated intraocular pressure and cataract are significant complications,[57,58,107] and care must be given to monitor for delayed glaucoma and optic nerve damage. More recently, investigators have considered intravitreal dexamethasone, with the advantage of shorter duration and perhaps fewer complications.

With the introduction of anti-VEGF therapy, combination therapy with PDT has also been studied. Experimental data suggested that intravitreal ranibizumab plus PDT caused a greater reduction in angiographic leakage than PDT and vehicle injection (PDT only).[109] Combination therapy trials include the combination of PDT and pegaptanib (Macugen) and PDT and ranibizumab (Lucentis). Comparison of ranibizumab alone vs PDT plus ranibizumab in the RhuFab V2 Ocular Treatment Combining the Use of Visudyne™ to Evaluate Safety (FOCUS) trial found no benefit to the combination therapy, although the results were clouded, since most enrolled patients had already undergone therapy (P. Lanzetta, MD, AAO Subspecialty Day, 2007). So-called triple therapy has been advocated by Augustin and others,[110] who have utilized PDT, intravitreal triamcinolone, and bevacizumab (Avastin) with promising results.

Several groups are studying combination therapy using reduced fluence PDT. The VIM trial, described above, changed 2 parameters—irradiance, or fluence rate, and fluence—and showed no improvement over standard PDT. However, one potential advantage to reduced fluence PDT would be to decrease the risk of treatment-related vision loss in patients with early lesions and better vision. These reduced fluence trials include a double-masked Phase 3b, multicenter randomized trial of combination Lucentis and PDT vs Lucentis montherapy (DENALI).

Another pathway to target in combination therapy is apoptosis. Early studies demonstrated the role of apoptosis in PDT-induced damage to CNV as well as unwanted damage to the outer retina, including photoreceptors. Apoptosis occurs as a direct effect on photoreceptors and endothelial cells through mediators like Akt as well as indirectly through activation of inflammatory cells.[50,51] The role of antiapoptotic agents in PDT of CNV would be to preserve photoreceptors while permitting or even augmenting apoptosis in CNV.

Targeting PDT more specifically to the endothelial cells of CNV is another approach to increase selectivity and improve vision results. Work by Renno and colleagues[45] demonstrated the effectiveness of verteporfin bound to a peptide directed at the VEGFR2 or VEGF receptor. Closure of CNV was possible at reduced drug and light doses, and damage to photoreceptors and RPE was barely detectable.

SUMMARY

Photodynamic therapy with verteporfin was the first pharmacologic therapy for neovascular AMD. It was successful in limiting vision loss in a substantial number of patients and could improve vision in a select few. The experimental work in the nonhuman primate was essential in developing treatment parameters that could successfully occlude CNV with limited injury to neural retina. A key element of that work was the demonstration of the safety of higher irradiance in this ocular application. Verteporfin PDT changed the treatment paradigm of neovascular AMD and CNV secondary to other causes, including pathologic myopia, POHS, and other inflammatory conditions. Subsequently, anti-VEGF therapy, particularly ranibizumab, has greatly improved treatment outcomes, with nearly all treated patients avoiding moderate vision loss and a substantial proportion showing 3-line vision improvement. Considerations in future treatments of neovascular AMD include how best to combine therapies, whether to alter dosing regimens, and how to time combination therapies to achieve synergy. These future therapies will include those yet untested, especially those targeting other pathways, such as apoptosis, inflammation, and other mediators of angiogenesis, including endostatin and angiostatin.

ACKNOWLEGMENTS

Funding/Support: QLT provided benzoporphyrin derivative (BPD) and later verteporfin as well as partial research support for the preclinical studies and subsequently (with CIBAVision/Novartis) support of the clinical trials. Research studies were supported at different times by the Massachusetts Lions Eye Research Fund, Research to Prevent Blindness Foundation, Massachusetts Eye and Ear Infirmary Foundation funding, Department of Energy grant FG02-91ER61228, Alcon Research Institute Award, and Macula Society Research Awards.

Financial Disclosures: The Massachusetts Eye and Ear Infirmary has an ownership interest in several US patents directed to the use of verteporfin. In addition, the Massachusetts Eye and Ear Infirmary has an ownership interest in certain patent applications directed to the selective destruction of subretinal choroidal neovasculature for the treatment of macular degeneration and other disorders. Should the Massachusetts Eye and Ear Infirmary receive royalties or other financial remunerations as a result of these patents and patent applications, Dr Miller would receive a share of the same in accordance with the Massachusetts Eye and Ear Infirmary's institutional patent policy and procedures, which includes royalty-sharing provisions. In addition, Dr Miller has served as an ad hoc consultant for Genentech, Inc, Bausch & Lomb, and Genzyme.

Conformity With Author Information: All animal experiments were carried out under the guidelines established by the Association for Research in Vision and Ophthalmology and used protocols approved by the Animal Care Committee of the Massachusetts Eye and Ear Infirmary.

Other Acknowledgments **(**This is a partial listing. Others are acknowledged in the cited references. Unless otherwise noted, all contributors listed below were affiliated with Massachusetts Eye and Ear Infirmary while working on these projects. Clinical studies involved multiple investigators who enrolled and treated patients, reviewed data, and contributed to the manuscripts.):

Contributions to AOS Thesis: Anne Marie Lane, MPH, provided significant help with writing and editing of this manuscript and, during the development of PDT, provided analysis of early clinical data, writing, and review of manuscripts. Ed Connolly, BS, helped with editing and image preparation for this manuscript and provided technical assistance through nearly all of the preclinical work as well as during the clinical trials. Norman Michaud, MS, helped with editing of this manuscript, image preparation, and histologic analysis and description, and in the preclinical studies, including the higher irradiance experiments, performed all of the histologic sectioning preparation and provided input into the findings. William Corcoran helped with assembling the data.

Contributions to Higher Irradiance Experiments: Rachel Moulton, DVM, provided technical assistance for much of the preclinical work including the higher irradiance experiments. Arthur Walsh, MD, performed the early preclinical experiments using BPD and DMSO under my direction, including the higher irradiance experiments. Thomas Flotte, MD, Massachusetts General Hospital, provided pathology expertise in the preclinical studies, including the higher irradiance experiments. Evangelos S. Gragoudas, MD, helped design the preclinical experiments and clinical trials, reviewed data, and provided critical review of manuscripts. Tayyaba Hasan, PhD, Massachusetts General Hospital, collaborated on early preclinical studies.

Other Contributions: Michal Kramer, MD, performed much of the preclinical experiments under my direction, particularly the liposomal studies, and the angiography. Francois Delori, PhD, Schepens Eye Research Institute, was an important contributor to photosensitizer angiography work. Robert Haimovici, MD, performed preclinical experiments under my direction including rabbit localization studies. Deeba Husain, MD, performed preclinical experiments using verteporfin under my direction including angiography, infusion studies, and long-term studies.

REFERENCES

1. Nanda S, Hatchell D, Tiedeman J, Dutton J, Hatchell M, McAdoo T. A new method of vascular occlusion. Photochemical initiation of thrombosis. *Arch Ophthalmol* 1987;105:1121-1124.
2. Miller JW, Stinson WG, Gregory WA, El-Khoumy HA, Puliafito CA. Phthalocyanine photodynamic therapy of experimental iris neovascularization. *Ophthalmology* 1991;98:1711-1719.
3. Kliman G, Puliafito C, Stern D, Borirakchanyavat S, Gregory W. Phthaloycyanine photodynamic therapy: new strategy for closure of choroidal neovascularization. *Lasers Surg Med* 1994;15:2-10.
4. Kliman G, Puliafito C, Grossman G, Gregory W. Retinal and choroidal vessel closure using phthalocyanine photodynamic therapy. *Lasers Surg Med* 1994;15:11-18.
5. Miller H, Miller B. Photodynamic therapy of subretinal neovascularization in the monkey eye. *Arch Ophthalmol* 1993;111:855-860.
6. Reinke MH, Canakis C, Husain D, et al. Verteporfin photodynamic therapy retreatment of normal retina and choroid in the cynomolgus monkey. *Ophthalmology* 1999;106:1915-1923.
7. Miller JW, Walsh AW, Kramer M, et al. Photodynamic therapy of experimental choroidal neovascularization using lipoprotein-delivered benzoporphyrin. *Arch Ophthalmol* 1995;113:810-818.
8. Kramer M, Miller J, Michaud N, et al. Lipsomal BPD verteporfin photodynamic therapy: Selective treatment of choroidal neovascularization in monkeys. *Ophthalmology* 1996;103:427-438.
9. Husain D, Miller J, Michaud N, Connolly E, Flotte T, Graoudas E. Intravenous infusion using liposomal benzoporphyrin derivative verteporfin for photodynamic therapy of experimental choroidal neovascularization. *Arch Ophthalmol* 1996;114:978-985.
10. Husain D, Miller J, Kenney A, Michaud N, Flotte T, Gragroudas E. Photodynamic therapy and digital angiography of experimental iris neovascularization using liposomal benzoporphyrin derivative. *Ophthalmology* 1997;104:1242-1250.
11. Husain D, Kramer M, Kenny AG, et al. Effects of photodynamic therapy using verteporfin on experimental choroidal neovascularization and normal retina and choroid up to 7 weeks after treatment. *Invest Ophthalmol Vis Sci* 1999;40:2322-2331.
12. van den Bergh HE, Ballini JP. Principles of photodynamic therapy. In: Gragoudas ES, Miller JW, Zografos L, eds. *Photodynamic Therapy of Ocular Diseases*. Philadelphia: Lippincott, Williams & Wilkins; 2004:11-42.
13. Svaasand L, Ellingson R. Optical properties of human brain. *Photochem Photobiol* 1983;38:283-289.
14. Hasan T, Parish J. Photodynamic therapy of cancer. In: Holland J, ed. *Cancer Medicine*. 4th ed. Baltimore: Williams & Wilkins; 1997:739-751.
15. Figge F, Weiland G, Manganiello L, et al. Cancer detection and and therapy. Affinity of neoplastic, embryonic and traumatized tissues for porphyrins and metalloporphyrins. *Proc Soc Exp Biol Med* 1948;68:640-641.
16. Kongshaug M. Distribution of tetrapyrrole photosensitizers among human plasma proteins. *Int J Biochem* 1992;24:1239-1265.
17. Jori G, Beltramini M, Reddi E, et al. Evidence for a major role of plasma lipoproteins as hematoporphyrin carriers in vivo. *Cancer Lett* 1984;24:291-297.
18. Ginevra F, Biffanti S, Pagnan A, Biolo R, Reddi E, Jori G. Delivery of the tumour photosensitizer zinc(II)-phthalocyanine to serum proteins by different liposomes: studies in vitro and in vivo. *Cancer Lett* 1990;49:59-65.
19. Jori G, Reddi E. The role of lipoproteins in the delivery of tumour-targeting photosensitizers. *Int J Biochem* 1993;25:1369-1375.
20. Allison B, Pritchard P, Richter A, Levy J. The plasma distribution of benzoporphyrin derivative and the effects of plasma lipoproteins on its biodistribution. *Photochem Photobiol* 1990;52:501-507.

21. Polo L, Reddi E, Garbo GM, Morgan AR, Jori G. The distribution of the tumour photosensitizers Zn(II)-phthalocyanine and Sn(IV)-etiopurpurin among rabbit plasma proteins. *Cancer Lett* 1992;66:217-223.
22. Kessel D. Photosensitization of neoplastic tissues with derivatives of hematoporphyrin. *Photodermatol* 1989;6:197-199.
23. Jori G. Low density lipoprotein-liposome delivery system for tumor photosensitizers in vivo. In: Henderson B, Dougherty T, eds. *Photodynamic Therapy, Basic Principles and Clinical Applications*. New York: Dekker; 1992:173-186.
24. Kessel D, Chang CK, Henderson BW. Photosensitization with methylene-linked porphyrin dimers. *J Photochem Photobiol B* 1993;18:177-180.
25. Gaffney J, West D, Arnold F, Sattar A, Kumar S. Differences in the uptake of modified low density lipoproteins by tissue cultured endothelial cells. *J Cell Sci* 1985;79:317-325.
26. Ricchelli F, Gobbo S, Jori G, Moreno G, Vinzens F, Salet C. Photosensitization of mitochondria by liposome-bound porphyrins. *Photochem Photobiol* 1993;58:53-58.
27. Dougherty TJ, Gomer CJ, Henderson BW, et al. Photodynamic therapy. *J Natl Cancer Inst* 1998;90:889-905.
28. Jori G, Tomio L, Reddi E, et al. Preferential delivery of liposome-incorporated porphryin to neoplastic cells in tumour-bearing rats. *Br J Cancer* 1983;48:307-309.
29. Allison BA, Waterfield E, Richter AM, Levy JG. The effects of plasma lipoproteins on in vitro tumor cell killing and in vivo tumor photosensitization with benzoporphyrin derivative. *Photochem Photobiol* 1991;54:709-715.
30. Barel A, Jori G, Perin A, Romandini P, Pagnan A, Biffanti S. Role of high-, low-, and very low-density lipoproteins in the transport and tumor-delivery of hematoporphyrin in vivo. *Cancer Lett* 1986;32:145-150.
31. Allison B, Pritchard P, Levy J. Evidence for low-density lipoprotein receptor-mediated uptake of benzoporphyrin derivative. *Br J Cancer* 1994;69:833-839.
32. Jori G, Beltramini M, Reddi E, et al. Evidence for a major role of plasma lipoproteins as hematoporphyrin carriers in vivo. *Cancer Lett* 1984;24:291-297.
33. West CML, West DC, Kumar S, Moore JV. A comparison of the sensitivity to photodynamic treatment of endothelial and tumour cells in different proliferative states. *Int J Radiat Biol* 1990;58:145-156.
34. Kessel D. Porphryin-lipoprotein association as a factor in porphyrin localization. *Cancer Lett* 1986;33:183-188.
35. Hamblin MR, Newman EL. Photosensitizer targeting in photodynamic therapy. II. Conjugates of haematoporphyrin with serum lipoproteins. *J Photochem Photobiol B* 1994;26:147-157.
36. Dunn KC, Marmorstein AD, Bonilha VL, Rodriguez-Boulan E, Giordano F, Hjelmeland LM. Use of the ARPE-19 cell line as a model of RPE polarity: basolateral secretion of FGF5. *Invest Ophthalmol Vis Sci* 1998;39:2744-2749.
37. Nguyen-Legros J, Hicks D. Renewal of photoreceptor outer segments and their phagocytosis by the retinal pigment epithelium. *Int Rev Cytol* 2000;196:245-313.
38. Noske UM, Schmidt-Erfurth U, Meyer C, Diddens H. Lipid metabolism in retinal pigment epithelium. Possible significance of lipoprotein receptors. *Ophthalmologe* 1998;95:814-819.
39. Schmidt-Erfurth U, Bauman W, Gragoudas E, et al. Photodynamic therapy of experimental choroidal melanoma using lipoprotein-delivered benzoporphyrin. *Ophthalmology* 1994;101:89-99.
40. Henderson B, Dougherty T. How does photodynamic therapy work? *Photochem Photobiol* 1992;55:931-948.
41. Jiang F, Allison B, Liu D, Levy J. Enhanced photodynamic killing of target cells by either monoclonal antibody or low density lipoprotein mediated delivery systems. *J Control Release* 1992;19:41-58.
42. Mew D, Wat CK, Towers GH, Levy JG. Photoimmunotherapy: treatment of animal tumors with tumor-specific monoclonal antibody-hematoporphyrin conjugates. *J Immunol* 1983;130:1473-1477.
43. Goff BA, Bamberg M, Hasan T. Photoimmunotherapy of human ovarian carcinoma cells ex vivo. *Cancer Res* 1991;51:4762-4767.
44. Hu LK, Hasan T, Gragoudas ES, Young LH. Photoimmunotherapy of human uveal melanoma cells. *Exp Eye Res* 1995;61:385-391.
45. Renno RZ, Terada Y, Haddadin MJ, Michaud NA, Gragoudas ES, Miller JW. Selective photodynamic therapy by targeted verteporfin delivery to experimental choroidal neovascularization mediated by a homing peptide to vascular endothelial growth factor receptor-2. *Arch Ophthalmol* 2004;122:1002-1011.
46. Binetruy-Tournaire R, Demangel C, Malavaud B, et al. Identification of a peptide blocking vascular endothelial growth factor (VEGF)-mediated angiogenesis. *Embo J* 2000;19:1525-1533.
47. Nelson J, Liaw L, Orenstein A, Roberts W, Berns M. Mechanism of tumor destruction following photodynamic therapy with hematoporphyrin derivative, chlorin, and phthalocyanine. *J Natl Cancer Inst* 1988;80:1599-1605.
48. Berg K, Moan J. Lysosomes and microtubules as targets for photochemotherapy of cancer. *Photochem Photobiol* 1997;65:403-409.
49. Fingar V. Vascular effect of photodynamic therapy. *J Clin Laser Med Surg* 1996;14:323-328.
50. Matsubara A, Nakazawa T, Noda K, et al. Photodynamic therapy induces caspase-dependent apoptosis in rat CNV model. *Invest Ophthalmol Vis Sci* 2007;48:4741-4747.
51. She H, Nakazawa T, Matsubara A, et al. Reduced photoreceptor damage after photodynamic therapy through blockade of nitric oxide synthase in a model of choroidal neovascularization. *Invest Ophthalmol Vis Sci* 2007;48:2268-2277.

52. Ju WK, Chung IW, Kim KY, et al. Sodium nitroprusside selectively induces apoptotic cell death in the outer retina of the rat. *Neuroreport* 2001;12:4075-4079.
53. Osborne NN, Wood JP. Metipranolol blunts nitric oxide-induced lipid peroxidation and death of retinal photoreceptors: a comparison with other anti-glaucoma drugs. *Invest Ophthalmol Vis Sci* 2004;45:3787-3795.
54. Donovan M, Carmody RJ, Cotter TG. Light-induced photoreceptor apoptosis in vivo requires neuronal nitric-oxide synthase and guanylate cyclase activity and is caspase-3-independent. *J Biol Chem* 2001;276:23000-23008.
55. Chan WM, Lai TY, Wong AL, Tong JP, Liu DT, Lam DS. Combined photodynamic therapy and intravitreal triamcinolone injection for the treatment of subfoveal choroidal neovascularisation in age related macular degeneration: a comparative study. *Br J Ophthalmol* 2006;90:337-341.
56. Spaide RF, Sorenson J, Maranan L. Combined photodynamic therapy with verteporfin and intravitreal triamcinolone acetonide for choroidal neovascularization. *Ophthalmology* 2003;110:1517-1525.
57. Arias L, Garcia-Arumi J, Ramon JM, Badia M, Rubio M, Pujol O. Photodynamic therapy with intravitreal triamcinolone in predominantly classic choroidal neovascularization: one-year results of a randomized study. *Ophthalmology* 2006;113:2243-2250.
58. Augustin AJ, Schmidt-Erfurth U. Verteporfin and intravitreal triamcinolone acetonide combination therapy for occult choroidal neovascularization in age-related macular degeneration. *Am J Ophthalmol* 2006;141:638-645.
59. Chaudhary V, Mao A, Hooper PL, Sheidow TG. Triamcinolone acetonide as adjunctive treatment to verteporfin in neovascular age-related macular degeneration: a prospective randomized trial. *Ophthalmology* 2007;114:2183-2189.
60. Bonnet R, Ridge R, Scourides P, et al. On the nature of hematoporphyrin derivative. *J Chem Soc [Perkin 1]* 1981;1:3135-3140.
61. Davidorf J, Davidorf F. Treatment of iris melanoma with photodynamic therapy. *Ophthalmic Surg* 1992;23:522-527.
62. Levy J. Photosensitizers in photodynamic therapy. *Semin Oncol* 1994;21:4-10.
63. Kato H, Horai T, Furuse K, et al. Photodynamic therapy of cancers: a clinical trial of porfimer sodium in Japan. *Jpn J Cancer Res* 1993;84:1209-1214.
64. Nelson JS, Roberts WG, Berns MW. In vivo studies on the utilization of mono-l-aspartyl chlorin (NPe6) for photodynamic therapy. *Cancer Res* 1987;47:4681-4685.
65. Schuitmaker J, van Best J, van Delft J, Dubbelman T, Oosterhuis J, de Wolff-Rouendaal D. Bacteriochlorin a, a new photosensitizer in photodynamic therapy In vivo results. *Invest Ophthalmol Vis Sci* 1990;31:1444-1450.
66. Richter AM, Waterfield E, Jain AK, et al. Photosensitising potency of structural analogues of benzoporphyrin derivative (BPD) in a mouse tumour model. *Br J Cancer* 1991;63:87-93.
67. Moshfeghi DM, Peyman GA. Photodynamic therapy for experimental choroidal neovascularization using purlytin. In: Gragoudas ES, Miller JW, Zografos L, eds. *Photodynamic Therapy of Ocular Diseases*. Philadelphia: Lippincott, Williams & Wilkins; 2004:85-88.
68. Thomas EL, Snyder WJ. Photodynamic therapy with tin ethyl etiopurpurin. In: Gragoudas ES, Miller JW, Zografos L, eds. *Photodynamic Therapy of Ocular Diseases*. Philadelphia: Lippincott, Williams & Wilkins; 2004:231-237.
69. Kazi AA, Peyman GA, Unal M, et al. Threshold power levels for NPe6 photodynamic therapy. *Ophthalmic Surg Lasers* 2000;31:136-142.
70. Obana A, Gohto Y, Kaneda K, Nakajima S, Miki T. PDT to monkey CNV with ATX-S10(Na): inappropriateness of early laser irradiation for selective occlusion. *Invest Ophthalmol Vis Sci* 2001;42:2639-2645.
71. Obana A, Gohto Y, Kanai M, Nakajima S, Kaneda K, Miki T. Selective photodynamic effects of the new photosensitizer ATX-S10(Na) on choroidal neovascularization in monkeys. *Arch Ophthalmol* 2000;118:650-658.
72. Obana A. Photodynamic therapy for experimental choroidal neovascularization using ATX-S10(Na). In: Gragoudas ES, Miller JW, Zografos L, eds. *Photodynamic Therapy of Ocular Diseases*. Philadelphia: Lippincott, Williams & Wilkins; 2004:73-83.
73. Kreimer-Birnbaum M. Modified porphyrins, chlorins, phthalocyanines, and purpurins: second-generation photosensitizers for photodynamic therapy. *Semin Hematol* 1989;26:157-173.
74. Morgan A, Skalkos D. Second generation sensitizers: where are we and where should we be going? *Proc Soc Photo Opt Instrum Eng* 1990;6:87-106.
75. Panagopoulos JA, Svitra PP, Puliafito CA, Gragoudas ES. Photodynamic therapy for experimental intraocular melanoma using chloraluminum sulfonated phthalocyanine. *Arch Ophthalmol* 1989;107:886-890.
76. Woodburn K, Fan Q, Kessel D, et al. Phototherapy of cancer and atheromatous plaque with texaphyrins. *J Clin Laser Med Surg* 1996;14:343-348.
77. Woodburn K, Fan Q, Miles D, Kessel D, Luo Y, Young S. Localization and efficacy analysis of the phototherapeutic lutetium texaphyrin (PCI-0123) in the murine EMT6 sarcoma model. *Photochem Photobiol* 1997;65:410-415.
78. Arbour JD, Gauthier D. Photodynamic therapy for experimental neovascularization using Lu-Tex. In: Gragoudas ES, Miller JW, Zografos L, eds. *Photodynamic Therapy of Ocular Diseases*. Philadelphia: Lippincott, Williams & Wilkins; 2004:89-97.
79. Blumenkranz MS, Woodburn K, Miller JW, Slakter JS. Photodynamic therapy with Lu-Tex: Early results. In: Gragoudas ES, Miller JW, Zografos L, eds. *Photodynamic Therapy of Ocular Diseases*. Philadelphia: Lippincott, Williams & Wilkins; 2004:239-248.
80. Yoshikawa K, Kurata H, Iwahara S, Kada T. Photodynamic action of fluorescein dyes in DNA-damage and in vitro inactivation of transforming DNA in bacteria. *Mutat Res* 1978;56:359-362.

81. Gandin E, Lion Y, Van De Vorst A. Quantum yield of singlet oxygen production by xanthene derivatives. *Photochem Photobiol* 1983;37:271-278.
82. Wilson C, Hatchell D. Photodynamic retinal vascular thrombosis. *Invest Ophthalmol Vis Sci* 1991;32:2357-2365.
83. Royster A, Nanda S, Hatchell D, Tiedeman J, Dutton J, Hatchell M. Photochemical initiation of thrombosis. Fluorescein angiographic, histologic, and ultrastructural alterations in the choroid, retinal pigment epithelium, and retina. *Arch Ophthalmol* 1988;106:1608-1614.
84. Liu H, Anderson R. Photodynamic therapy in dermatology: recent developments. *Dermatol Clin* 1993;11:1-13.
85. Rudel LL, Lee JA, Morris MD, Felts JM. Characterization of plasma lipoproteins separated and purified by agarose-column chromatography. *Biochem J* 1974;139:89-95.
86. Haimovici R, Kramer M, Miller J, et al. Localization of lipoprotein-delivered benzoporphyrin derivative in the rabbit eye. *Curr Eye Res* 1997;16:83-90.
87. Waldow S, Dougherty T. Interaction of hyperthermia and photoradiation therapy. *Radiat Res* 1984;97:380-385.
88. Miller J, Schmidt-Erfurth U, Sickenberg M, et al. Photodynamic therapy with verteporfin for choroidal neovascularization caused by age-related macular degeneration. Results of a single treatment in a Phase 1 and 2 study. *Arch Ophthalmol* 1999;117:1161-1173.
89. Renno R, Delori F, Holzer R, Gragoudas E, Miller J. Photodynamic therapy using Lu-Tex induces apoptosis in vitro, and its effect is potentiated by angiostatin in retinal capillary endothelial cells. *Invest Ophthalmol Vis Sci* 2000;41:3963-3971.
90. Zacks D, Ezra E, Terada Y, et al. Verteporfin photodynamic therapy in the rat model of choroidal neovascularization: angiographic and histologic characterization. *Invest Ophthalmol Vis Sci* 2002;43:2384-2391.
91. She H, Nakazawa T, Matsubara A, et al. Dexamethasone reduces photoreceptor damage caused by photodynamic therapy in a rat model of choroidal neovascularization. *Invest Ophthalmol Vis Sci* [published online ahread of print April 17, 2008] doi:10.1167/iovs.07-1154.
92. Richter AM, Waterfield E, Jain AK, Sternberg ED, Dolphin D, Levy JG. In vitro evaluation of phototoxic properties of four structurally related benzoporphyrin derivatives. *Photochem Photobiol* 1990;52:495-500.
93. Kessel D. In vitro photosensitization with a benzoporphryin derivative. *Photochem Photobiol* 1989;49:579-582.
94. Husain D, Kramer M, Gragoudas ES, Miller JW. Angiography with verteporfin. In: Gragoudas ES, Miller JW, Zografos L, eds. *Photodynamic Therapy of Ocular Diseases*. Philadelphia: Lippincott, Williams & Wilkins; 2004:249-253.
95. Husain D, Gragoudas ES, Miller JW. Photodynamic therapy. In: Albert DM, Miller JW, eds. *Albert and Jakobiec's Principles and Practice of Ophthalmology*. 3rd ed. Philadelphia: Saunders Elsevier; 2008:1953-1961.
96. Treatment of Age-related Macular Degeneration with Photodynamic Therapy (TAP) Study Group. Verteporfin (Visudyne™) therapy of subfoveal choroidal neovascularization in age-related macular degeneration. One year results of two randomized clinical trials—TAP Report #1. *Arch Ophthalmol* 1999;117:1329-1345.
97. Treatment of Age-related Macular Degeneration with Photodynamic Therapy (TAP) Study Group. Photodynamic therapy of subfoveal choroidal neovascularization in age-related macular degeneration with verteporfin. Two-year vision results of two randomized clinical trials. TAP Report # 2. *Arch Ophthalmol* 2001;119:198-207.
98. Verteporfin therapy of subfoveal choroidal neovascularization in age-related macular degeneration: two-year results of a randomized clinical trial including lesions with occult with no classic choroidal neovascularization—verteporfin in photodynamic therapy report 2. *Am J Ophthalmol* 2001;131:541-560.
99. Bressler NM, Arnold J, Benchaboune M, et al. Verteporfin therapy of subfoveal choroidal neovascularization in patients with age-related macular degeneration: additional information regarding baseline lesion composition's impact on vision outcomes—TAP report No. 3. *Arch Ophthalmol* 2002;120:1443-1454.
100. Sickenberg M, Schmidt-Erfurth U, Miller JW, et al. A preliminary study of photodynamic therapy using verteporfin for choroidal neovascularization in pathologic myopia, ocular histoplasmosis syndrome, angioid streaks, and idiopathic causes. *Arch Ophthalmol* 2000;118:327-336.
101. Azab M, Boyer DS, Bressler NM, et al. Verteporfin therapy of subfoveal minimally classic choroidal neovascularization in age-related macular degeneration: 2-year results of a randomized clinical trial. *Arch Ophthalmol* 2005;123:448-457.
102. Rosenfeld PJ, Saperstein DA, Bressler NM, et al. Photodynamic therapy with verteporfin in ocular histoplasmosis: uncontrolled, open-label 2-year study. *Ophthalmology* 2004;111:1725-1733.
103. Saperstein DA, Rosenfeld PJ, Bressler NM, et al. Photodynamic therapy of subfoveal choroidal neovascularization with verteporfin in the ocular histoplasmosis syndrome: one-year results of an uncontrolled, prospective case series. *Ophthalmology* 2002;109:1499-1505.
104. Spaide RF, Freund KB, Slakter J, Sorenson J, Yannuzzi LA, Fisher Y. Treatment of subfoveal choroidal neovascularization associated with multifocal choroiditis and panuveitis with photodynamic therapy. *Retina* 2002;22:545-549.
105. Rogers AH, Duker JS, Nichols N, Baker BJ. Photodynamic therapy of idiopathic and inflammatory choroidal neovascularization in young adults. *Ophthalmology* 2003;110:1315-1320.
106. Rosenfeld PJ, Brown DM, Heier JS, et al. Ranibizumab for neovascular age-related macular degeneration. *N Engl J Med* 2006;355:1419-1431.
107. Rechtman E, Danis RP, Pratt LM, Harris A. Intravitreal triamcinolone with photodynamic therapy for subfoveal choroidal neovascularisation in age related macular degeneration. *Br J Ophthalmol* 2004;88:344-347.

108. Spaide RF, Sorenson J, Maranan L. Photodynamic therapy with verteporfin combined with intravitreal injection of triamcinolone acetonide for choroidal neovascularization. *Ophthalmology* 2005;112:301-304.
109. Husain D, Kim I, Gauthier D, et al. Safety and efficacy of intravitreal injection of ranibizumab in combination with verteporfin PDT on experimental choroidal neovascularization in the monkey. *Arch Ophthalmol* 2005;123:509-516.
110. Augustin AJ, Puls S, Offermann I. Triple therapy for choroidal neovascularization due to age-related macular degeneration: verteporfin PDT, bevacizumab, and dexamethasone. *Retina* 2007;27:133-140.